HORSE PLASMA VITAMIN D-BINDING PROTEIN: ISOLATION AND STRUCTURAL INVESTIGATION

By

ROBERT CHARLES ROBINSON

B.Sc. King's College, London University, 1987

A THESIS SUBMITTED IN PARTIAL FULFILLMENT

OF THE REQUIREMENTS FOR THE DEGREE OF

MASTER OF SCIENCE

IN

THE FACULTY OF GRADUATE STUDIES

(Department of Chemistry)

We accept this thesis as conforming

to the required standard

THE UNIVERSITY OF BRITISH COLUMBIA

OCTOBER 1990

In presenting this thesis in partial fulfilment of the requirements for an advanced degree at the University of British Columbia, I agree that the Library shall make it freely available for reference and study. I further agree that permission for extensive copying of this thesis for scholarly purposes may be granted by the head of my department or by his or her representatives. It is understood that copying or publication of this thesis for financial gain shall not be allowed without my written permission.

Department of CHEMISTRY

The University of British Columbia
Vancouver, Canada

Date 30/10/90

Abstract

Vitamin D-binding protein (DBP) is an abundant serum protein, secreted by the liver, which transports vitamin D sterols and is part of an actin scavenging system. In this study, DBP was isolated from horse plasma in a highly reproducible, four step procedure: Affi-gel Blue affinity chromatography, gel filtration, hydroxylapatite chromatography and anion exchange HPLC. 6-7 mg of DBP were obtained from 80 ml of plasma with a yield of 21-25%.

The secondary structure of DBP was calculated from circular dichroism measurements to be 39% α-helix, 42% β-sheet and 19% random coil. A molecular mass of 53,000 ± 3,000 daltons was calculated from electrophoretic gels. Circular dichroism and fluorescence studies revealed that the disulphide bonds of DBP contribute substantial structural stabilization to the molecule with respect to thermal denaturation.

Finally, acrylodan-labeled DBP was prepared. The fluorescence of this adduct was sensitive to the binding of actin and to the presence of dithiothreitol.

Table of Contents

	Page
Abstract	ii
List of Tables	vi
List of Figures	vii
Acknowledgements	x
Abbreviations	ix
1: Introduction	
Part 1: Proteins	
1.1.1 Functions of Actin	1
1.1.2 Actin Polymerization/Depolymerization	6
1.1.3 Actin Scavenging System in Plasma	8
1.1.4 Review of DBP	9
1.1.5 Physical Properties of DBP	11
1.1.6 Review of DBP Purification Methods	13
Part 2: Spectroscopic Techniques	
1.2.1 Protein Absorbance Spectroscopy	15
1.2.3 Protein Fluorescence Spectroscopy	18
1.2.3 Protein CD Spectroscopy	20

2: Materials and Methods

Part 1: Proteins

2.1.1 Preparation of G-actin 23

2.1.2 Preparation of Pyrene-actin 24

2.1.3 Preparation of Acrylodan-actin 24

2.1.4 Acrylodan-actin Assay 25

2.1.5 Collection of Horse Plasma 26

2.1.6 Purification of DBP 26

2.1.7 Calculation of an Extinction Coefficient for DBP 29

2.1.8 Preparation of Acrylodan-DBP 30

2.1.9 Gel Electrophoresis 30

Part 2: Spectroscopic Methods

2.2.1 Absorbance Spectra 31

2.2.2 Fluorescence Spectra 31

2.2.3 CD Spectra 31

3: Results and Discussion

Part 1: Yield and Purity of DBP

3.1.1 Yield and Purity 32

3.1.2 Optical Spectra 34

3.1.3 Actin Assays 37

3.1.4 Calculation of Molecular Mass 40

3.1 5 Calculation of Secondary Structure 42

Part 2: Stability of DBP

3.2.1 CD Thermal Denaturation 43

3.2.2 Fluorescence Thermal Denaturation 47

3.2.3 CD Guanadine.HCl Induced Denaturation 47

Part 3: Acrylodan-DBP

3.3.1 Acrylodan Labeling of DBP 50

3.3.2 Acrylodan-DBP/Actin Interaction 53

3.3.3 Effect of DTT on Fluorescence of Acrylodan Covalently Bound to DBP 54

Part 4: Conclusions 55

Bibliography 57

List of Tables

Table		Page
I	Physical Properties of DBP	11

List of Figures

		Page
1	The thin filament of skeletal muscle	1
2	The main components of skeletal muscle	2
3	The mechanism of muscle contraction	3
4	Immunofluorescence micrograph of a resting cell stained with a fluorescent antibody to actin	4
5	Immunofluorescence micrograph of a moving cell stained with a fluorescent antibody to actin	4
6	Schematic diagram of F-actin	6
7	Schematic diagram showing the various activities of actin binding proteins along with examples	7
8	Schematic diagram of the complexes formed on the addition of G-actin or F-actin to gelsolin and DBP	8
9	Homology between the disulphide-bonding patterns in rat albumin and the predicted amino acid sequence in rat DBP. Small circles show amino acids deleted in comparison to albumin	12
10	Absorbance spectra of the aromatic amino acids	16
11	Second derivative spectra of the aromatic amino acids in 6 M GuHCL, sodium phosphate, pH 6.8	16
12	Second derivative spectrum of human serum albumin in GuHCl at arbitrary concentration	17
13	Fluorescence spectra of the aromatic acids excitation 278 nm	19
14	6-acryloyl-2-dimethylaminonaphthalene	19
15	N-(1-Pyrene)iodoacetamide	19
16	CD spectra of poly-L-lysine in the 1, α-helical; 2, β-sheet; 3, random coil conformations	21
17	Elution profile from HPLC column	32
18	SDS polyacrylamide electrophoretic gel showing the purification of DBP	33

19a	Absorbance spectrum of DBP	34
19b	Absorbance spectrum of albumin	34
20	Second derivative absorbance spectrum of DBP	35
21	Fluorescence emission spectrum, excitation 278 nm, of DBP	36
22	The acrylodan-actin assay	37
23	Time related pyrene-actin fluorescence studies, excitation at 344 nm and emission at 386 nm	38
24	SDS polyacrylamide electrophoretic gel for the calculation of molecular mass	40
25	Graph showing the log of molecular mass against distance moved on a electrophoretic gel	41
26	CD spectrum of DBP	42
27	Melting curve of DBP, in high salt, followed by CD at 220 nm	44
28	Melting curve of DBP, in low salt, followed by CD at 220 nm	46
29	Melting curve of DBP followed by fluorescence emission at 307 nm excitationon at 278 nm	48
30	Guanidine.HCl denaturation of DBP followed by CD	49
31	Fluorescence spectra of acrylodan-DBP (5:1 labeled). A) Excitation spectrum, emission at 510 nm B) Emission spectrum, excitation at 365 nm	51
32	The effect of DTT on the emission spectrum of acrylodan-DBP (5:1 labeled), excitation at 365 nm	52
33	The effect of actin binding on the emission spectrum of acrylodan-DBP (0.35:1 labeled), excitation at 365 nm	53
34	The effect of DTT on the emission spectrum of acrylodan-DBP (0.35:1 labeled), excitation at 365 nm	54

The force that drives the water through the rocks
Drives my red blood; that dries the mouthing streams
Turns mine to wax.
And I am dumb to mouth unto my veins
How at the mountain spring the same mouth sucks.

The force that through the green fuse drives the flower.

Dylan Thomas

Acknowledgement

I would like to thank Dr. Dana Devine for the use of her PhastSystem and Dr. Leslie D. Burtnick for everything else.

Abbreviations

Acrylodan	6-acryloyl-2-(dimethylamino)naphthalene
ATP	Adenosine 5'-Triphosphate
CD	Circular Dichroism
CM-Sephadex	Carboxymethyl-Sephadex
DBP	Vitamin D-Binding Protein
DEAE-Sephadex	Diethylaminoethyl-Sephadex
DMF	*N*,*N*-Dimethylformamide
DMSO	Dimethylsulphoxide
DTT	Dithiothreitol
EGTA	Ethylenebis(oxyethylenenitrilo)-tetraacetic Acid
Gc	Group Specific Component of Plasma
HPLC	High Pressure Liquid Chromatography
MOPS	3-(*N*-morpholino)propanesulphonic Acid
PMSF	Phenylmethylsulphonyl Fluoride
PIA	*N*-(1-pyrene)iodoacetamide
SDS	Sodium Dodecyl Sulphate
TEMED	*N*,*N*,*N*',*N*'-Tetramethylethylenediamine
Tris	Tris(hydroxymethyl)methylamine
Buffer A	2 mM Tris-HCl, 0.2 mM $CaCl_2$, 0.2 mM ATP, 1.0 mM DTT, pH 7.6
Buffer B	30 mM Na Phosphate Buffer, 0.1%(w/v) Sodium Azide, 50 µM PMSF, pH 7.0
Buffer E	25 mM Tris-HCl, 194 mM glycine, 0.2 mM ATP, pH 8.4
Buffer H	150 mM KCl, 20 mM MOPS, 1 mM EGTA, pH 7.3

1: Introduction

Part 1: Proteins

1.1.1 Functions of Actin

Actin is one of the most abundant proteins in eukaryotic cells, often comprising up to 20% of total cell protein. It is a multiple functioned, highly conserved protein playing a major role in muscle contraction and in the structure and motility of non-muscle cells (Stryer, 1981). Actin, in conjunction with tropomyosin and the troponin complex, forms the thin filament of muscle (fig 1). These thin filaments interact with the myosin heads of the thick filaments causing contraction of the muscle (fig 2).

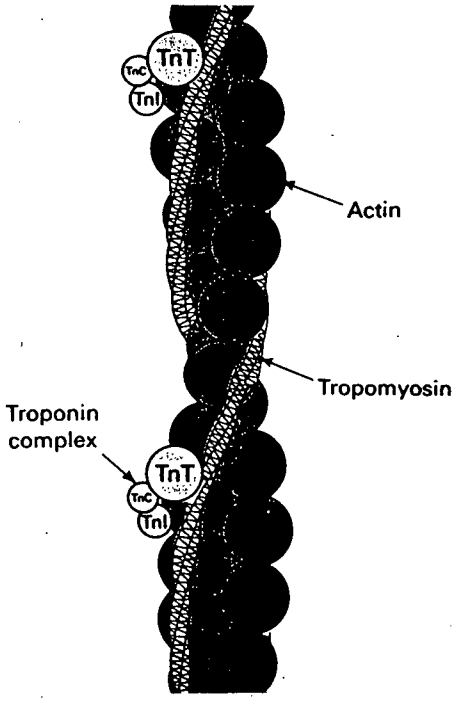

Fig 1: The thin filament of skeletal muscle. Stryer (1981).

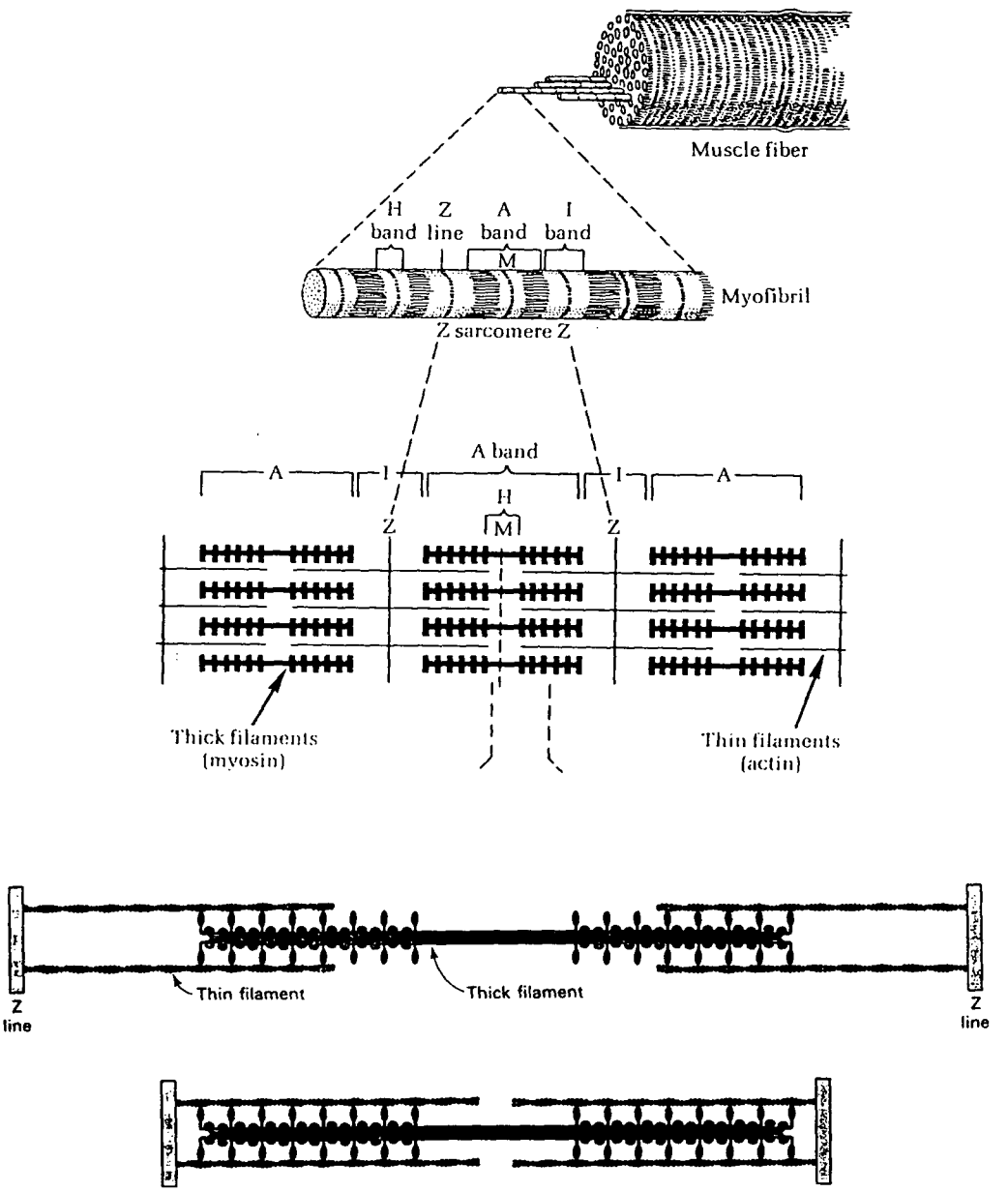

Fig 2: The main components of skeletal muscle. Lenhinger (1975).

The process is driven energetically by the hydrolysis of ATP to ADP. Myosin first binds to ATP (fig 3A) followed by myosin-ATP binding to actin (fig 3B). ATP then hydrolyses to ADP causing the myosin heads to tilt (fig 3C) resulting in the thick and thin filaments sliding over each other and consequently in the muscle contracting (fig 3D).

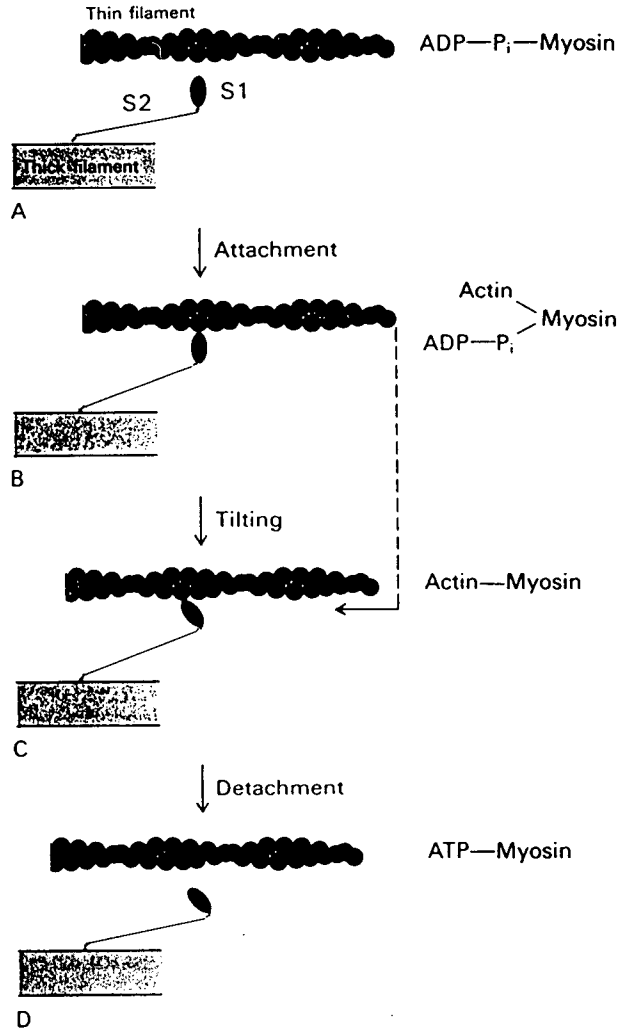

Fig 3: The mechanism of muscle contraction. Stryer (1981).

The control of contraction is provided through calcium ion regulation. Nerve pulses release calcium from the sarcoplasmic reticulum. This calcium binds to troponin C, which causes conformational changes that are transmitted to tropomyosin. These conformational changes in tropomyosin expose the necessary myosin binding sites on actin, allowing contraction to proceed.

Fig 4: Immunofluorescence micrograph of a resting cell stained with a fluorescent antibody to actin. Stryer (1981).

Fig 5: Immunofluorescence micrograph of a moving cell stained with a fluorescent antibody to actin. The ruffled border is the leading edge. Stryer (1981).

Actin is also a major constituent of non-muscle cells. Some of this actin forms microfilaments which resemble the thin filaments of muscle and contribute to the shape and structure of the cells (fig 4). By actively shortening these microfilaments in one direction and elongating them in the opposite direction the cell possesses the mechanism, through actin conformational changes, to move (fig 5).

The functions of actin outlined rely on its ability to polymerize and form filaments. In the case of muscle cells and contraction, the polymerization occurs just once. However it is a more transient affair in non-muscle cells where polymerization and depolymerization occur many times (Pollard and Craig, 1982).

1.1.2 Actin Polymerization/Depolymerization

Monomeric actin (G-actin) is a 42,000 dalton, globular protein and the polymer (F-actin) can be viewed in two ways (fig 6): as a double-stranded, right-handed helix with 13 actin units in each strand within each 72 nm helix pitch, or as a single-stranded, left-handed helix with a 5.9 nm pitch and 2.16 subunits per turn (Korn, 1982). G-actin can be polymerized spontaneously to F-actin in the presence of KCl or NaCl (50-150 mM) or $MgCl_2$ (0.5-2 mM). This polymerization is directional, occurring at both ends of a growing actin filament, but at two quite different rates. G-actin is favoured in the absence of salt and in the presence of ATP.

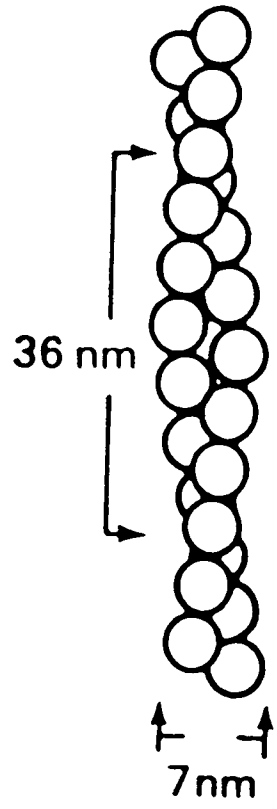

Fig 6: Schematic diagram of F-actin. Korn (1982).

The control of actin filament length via salt concentration is not specific enough to account for the variety of actin functions. Hence a series of actin binding proteins is found in cells which can modify the activity of actin (Way and Weeds, 1990). These actin binding proteins can be classified by their function (fig 7). Monomer binding proteins bind only to G-actin and, in the case of profilin, provide a buffering capacity for actin, ensuring that there is G-actin available for polymerization. Network and bundling proteins form F-actin aggregates, increasing the strength and diversity of actin structures. Finally the length of actin filaments can be regulated by severing and

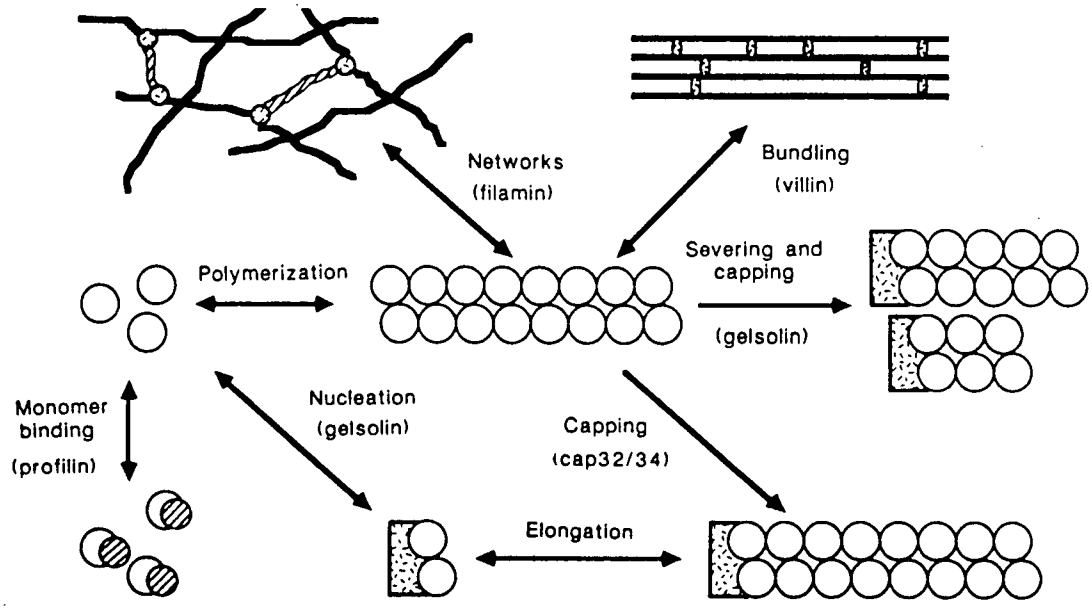

Fig 7: Schematic diagram showing the various activities of actin binding proteins along with examples. Way and Weeds (1990).

capping proteins which break up and slow down the polymerization, respectively, and by nucleation proteins which provide a foundation for rapid polymerization.

On the death of cells, whether the result of injury, disease or natural ageing, G-actin and F-actin are released into extracellular fluids, including blood plasma. The high salt conditions there favour F-actin and consequently could cause high plasma viscosity, blocking the microcirculation (Haddad et al., 1990). To avoid this fate, blood plasma possesses two F-actin depolymerizing proteins, gelsolin and DBP, which scavenge any actin released into the blood.

1.1.3 Actin Scavenging System in Plasma

Gelsolin is an F-actin severing protein with the ability to bind to either F-actin or G-actin. It has two actin-binding sites, one of which is calcium dependent. DBP is a monomer binding protein, forming a 1:1 complex with actin, K_a = 1-2 x 10^8 M^{-1} (Goldschmidt-Clermont et al., 1987). It can depolymerize F-actin indirectly by sequestering actin monomers, thus shifting the equilibrium away from F-actin. Janmey and Lind (1987) suggested that on the release of actin into blood, DBP binds the G-actin and gelsolin severs F-actin into short filaments. Further depolymerization of the gelsolin-capped actin filaments leads to the majority of actin being bound to DBP (fig 8).

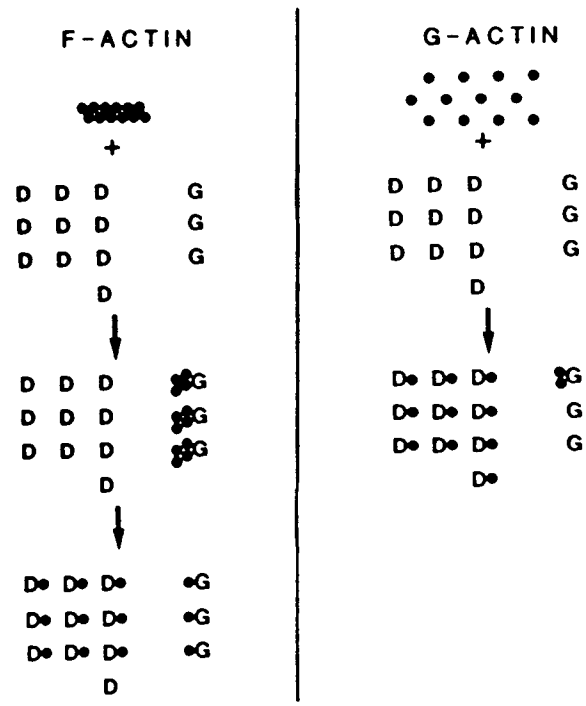

Fig 8: Schematic diagram of the complexes formed on the addition of G-actin or F-actin to gelsolin (G) and DBP (D). Janmey and Lind (1987).

This theory is supported by Coué et al. (1986) who found that, on addition of DBP and gelsolin to fluorescently labeled actin, only the DBP-actin complex was formed. In vitro studies using radiolabeled actin-binding proteins (Lind et al., 1986) showed that actin complexes of DBP and gelsolin are cleared from the plasma by the liver quicker than DBP or gelsolin alone, and that DBP-actin complexes are cleared faster than gelsolin-actin complexes. Furthermore Janmey et al. (1986) showed that DBP can remove an actin monomer from one of the two gelsolin binding sites, inferring that DBP is the main protein responsible for the disposal of extracellular actin as well as for rendering it inactive to polymerization.

1.1.4 Review of DBP

Hirschfeld (1959) discovered a postalbumin in human serum which migrated in the α_2 fraction on starch gel electrophoresis. He called this the Group Specific Component (Gc) System. In the same year, Thomas et al. reported a vitamin D-binding α-globulin, but it was not until 1975 that Daiger et al. showed Gc to be DBP. DBP since has been found in other body fluids such as urine, ascitic fluid and spinal fluid (Hirschfeld, 1962; Nielsen et al., 1963; Berggård et al., 1964).

DBP binds 1:1 to vitamin D with an affinity $K_a = 10^{10}\ M^{-1}$ at 4 °C (Bouillon et al. 1986) carrying out two functions; the transportation of vitamin D sterols as well as providing a circulating reservoir of the sterols (Cooke and Haddad, 1989).

However, the concentration of DBP (~5 x 10^{-6} M) is in vast excess of vitamin D (~5 x 10^{-8} M) in plasma, suggesting an alternate function. Although many thousands of sera have been tested for DBP, no deletion or gross alteration to the DBP gene has been found, implying that DBP has a vital role in plasma. Van Baelen et al. (1980) discovered DBP's actin-binding properties. Vitamin D and actin bind to DBP in a non-competitive manner.

DBP is synthesized in the liver at a rate of 10 mg kg^{-1} day^{-1} and is cleared from the circulation by the liver and kidneys. A radio-labeled DBP adduct, after intravenous injection, had a plasma $t_{\frac{1}{2}}$ of $1\frac{1}{2}$ hours whilst the complex of the adduct and actin had a plasma $t_{\frac{1}{2}}$ of 30 min (Dueland et al., 1990). Both the apo and holo vitamin D forms of DBP are cleared from plasma at the same rate (Cooke and Haddad, 1989). Other properties of DBP include binding fatty acids (Ena et al., 1989) and the 1:1 binding of calcium ions, which has been shown to be non-cooperative with actin binding (Goldschmidt-Clermont et al., 1987).

1.1.5 Physical Properties of DBP

Table I: Physical Properties of DBP

	M_r	Conc. in plasma
Man	59,000	10 µM
Mouse	49,000	———
Rat	52,000	9-13 µM

Some of the physical properties of DBP from different species are shown in table I. There is a large variance in molecular mass. On studying DBP from several species, Bouillon et al. (1986) suggested an average blood concentration of 300-400 mg/L species wide.

A rat DBP cDNA clone has been sequenced (Cooke, 1985) and has led to a predicted amino acid sequence for the protein (fig 9). The predicted sequence shows DBP to be of the same family of proteins as albumin. This family of proteins is thought to come from a common ancestral gene, with gene duplication occurring between 300-500 million years ago. Albumin shares some properties with DBP, such as the binding and transport of fatty acids, and albumin serves as a back up in the transport of steroid compounds (Stryer, 1981).

DBP is found to be rich in aspartic acid, glutamic acid and cysteine and low in glycine with no tryptophan residues. In rat DBP there are 28 cysteine residues which, due to the

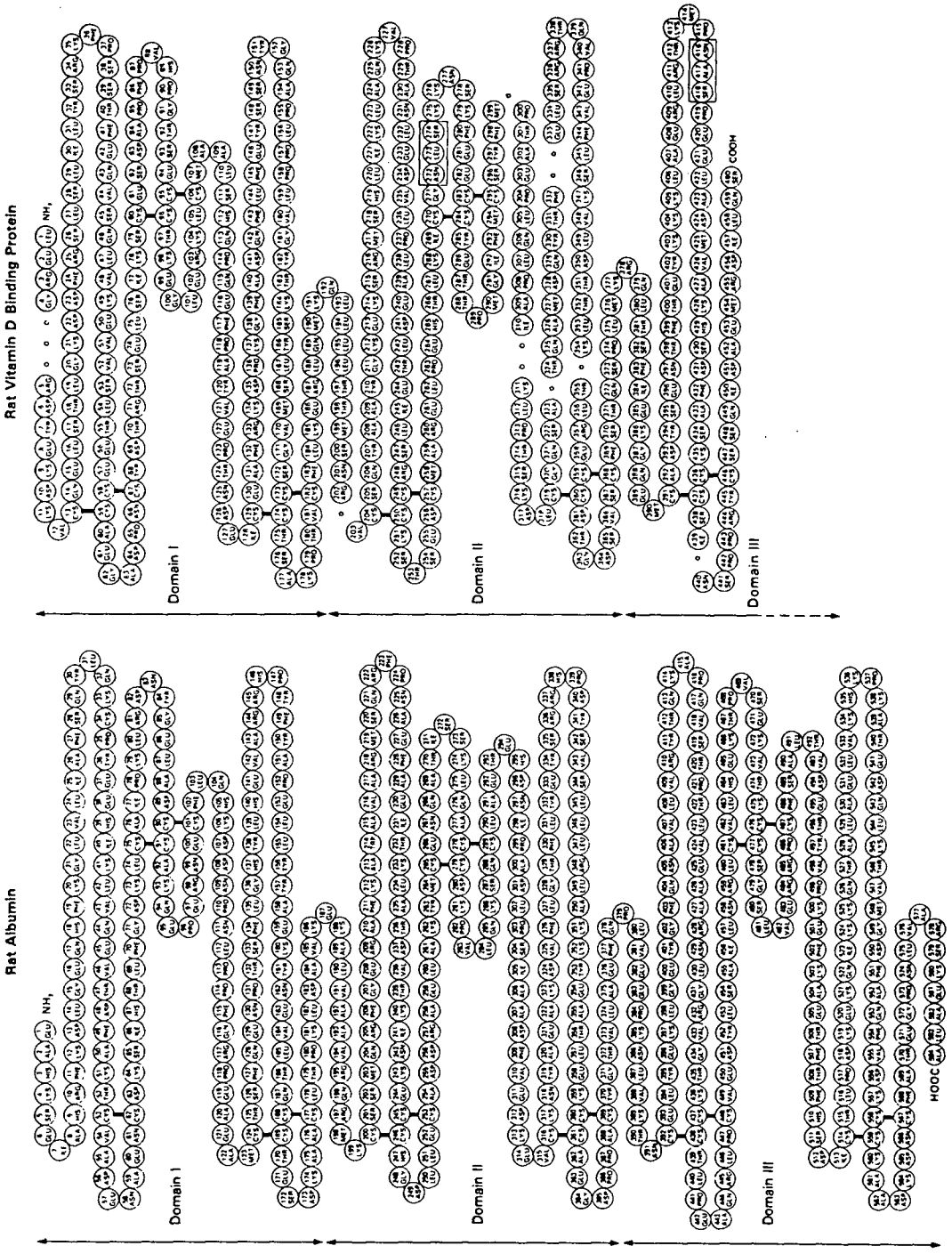

Fig 9: Homology between the disulphide-bonding patterns in rat albumin and the predicted amino acid sequence in rat DBP. Small circles show amino acids deleted in comparison to albumin. Cooke (1986).

similarity of the amino acid sequence to that of albumin (fig 9), have been proposed to all be involved in disulphide bonds (Cooke, 1985). This contrasts with earlier evidence from human DBP, where one deeply buried monothiol group was found (Kawakami and Goodmann, 1981).

DBP has proved useful in forensic science as it has many phenotypes and is relatively stable, able to survive 2 weeks at room temperature on dry cloth (Pötsch-Schneider and Klein, 1988). The DBP-vitamin D complex is found to be more stable than DBP alone (Kawakami and Goodmann, 1981).

1.1.6 Review of DBP Purification Methods

There have been many published purification schemes for DBP, most of which give poor yields due to the difficulty in separating DBP from albumin. A typical early method proposed by Bouillon et al. (1978) used 600 ml of rat serum and involved 7 steps: dialysis, DEAE-cellulose chromatography, precipitation with ammonium sulphate, hydroxylapatite chromatography, CM-cellulose chromatography, DEAE-Sephadex chromatography and gel filtration, with a final yield of 0.1%. In 1982, Chapuis-Cellier et al. utilized the high affinity of serum albumin for Affi-gel Blue (a trade name for cibacron blue dye covalently linked to agarose beads), in a three step procedure: Affi-gel Blue chromatography, gel filtration using Sephadex G-100 and DEAE-Affi-gel Blue chromatography to give a 73% yield with 97% purity from 80 ml of human plasma.

More recently, chromatographic methods using affinity matrices have been favoured despite their small capacity. Link et al. (1986) designed a vitamin D-Sepharose matrix, from which DBP could be removed by 60% acetone. When this step was followed by hydroxylapatite chromatography the overall yield was 55%. Finally, a DNAase I-Sepharose matrix was used to bind actin and then DBP. DBP was then eluted with 4 M $MgCl_2$ (van Baelen and Bouillon, 1986). Gel filtration served as a final purification step and provided a yield of 70% for human plasma DBP. This method has been employed for several different species but has produced contaminated material in some cases, including horse.

Part 2: Spectroscopic Techniques

1.2.1 Protein Absorbance Spectroscopy

Absorbance spectroscopy provides a convenient method of assessment of protein concentration as well as giving some clues to the amino acid composition of a protein.

Protein absorbance spectra in the wavelength region 250-320 nm are characteristic and are dominated by the contributions of three chromophores; tryptophan, tyrosine and phenylalanine. These absorbance spectra result from π to π^* electronic transitions in these aromatic systems.

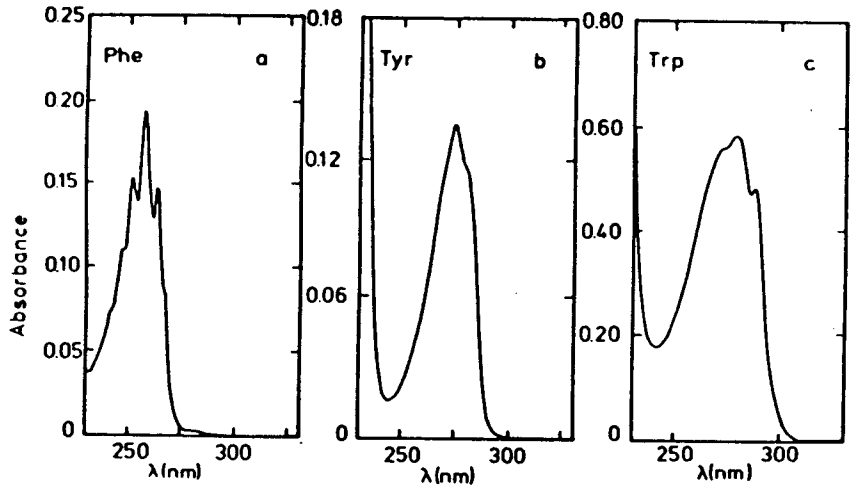

Fig 10: Absorbance spectra of the aromatic amino acids in a 1 cm cell in 0.01 M potassium phosphate buffer, pH 7.0 at 25° C. **a**, 1 mM phenylalanine; **b**, 0.1 mM tyrosine; **c**, 0.1 mM tryptophan. Creighton (1989).

Figure 10 shows the absorbance spectra of the isolated chromophores. Real protein absorbance spectra are the sum of all the individual chromophore absorbances.

A clearer method to identify the contributions of each of the chromophores to the protein absorbance spectrum is to look at the more distinctive second derivative spectra (fig 11). Clearly the contribution of tryptophan to the albumin (fig 12) spectrum can be identified. Albumin contains 1 tryptophan and 18 tyrosines.

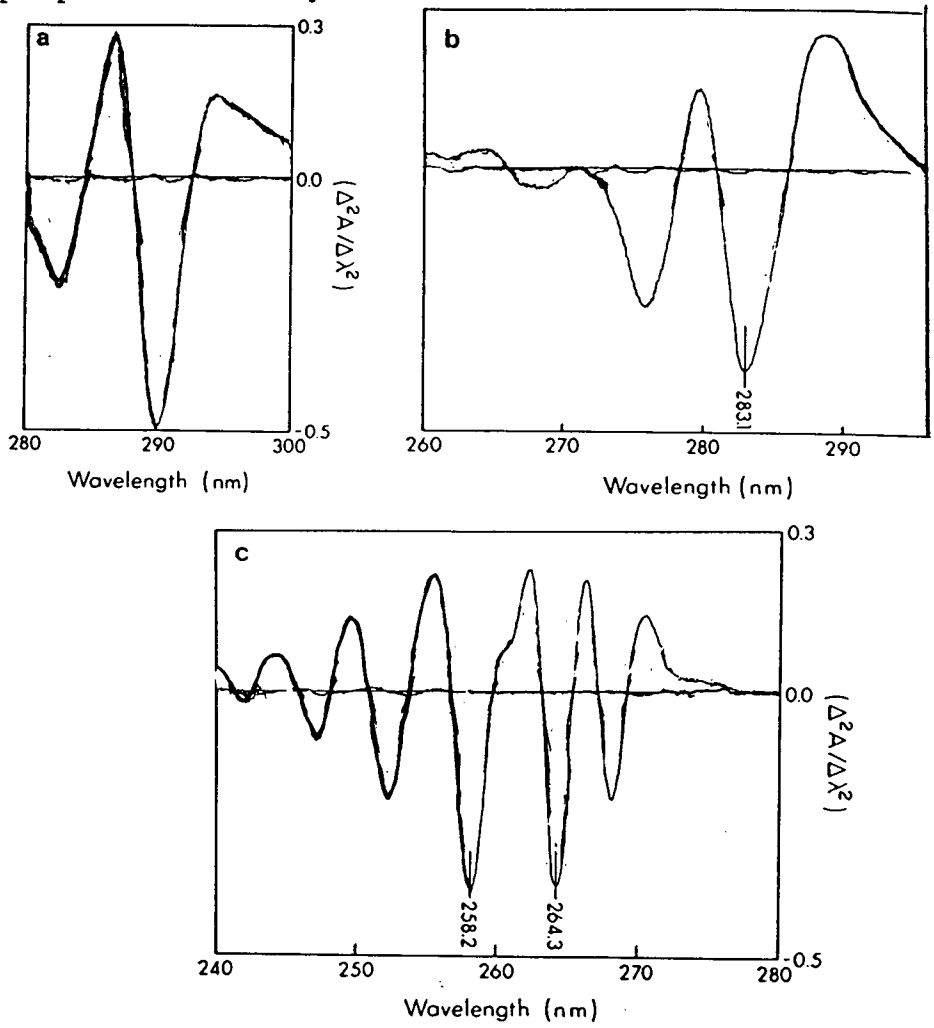

Fig 11: Second derivative spectra in 6 M GuHCL, sodium phosphate, pH 6.8. Nozaki (1990).
(a) $AcTrpNH_2$, 2.51 x 10^{-4} M,
(b) $AcTyrNH_2$, 7.6 x 10^{-4} M,
(c) AcPheOEt, 1.78 x 10^{-3} M.

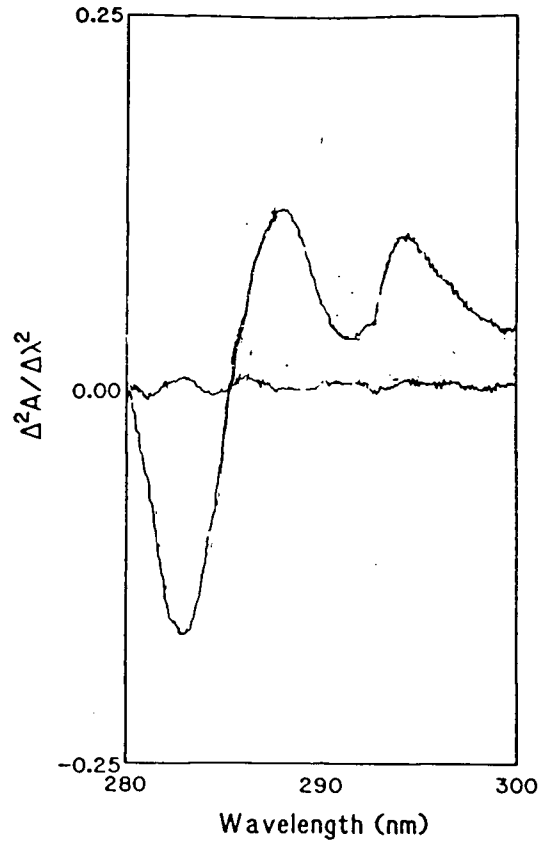

Fig 12: Second derivative spectrum of human serum albumin in GuHCl at arbitrary concentration. Nozoki (1990).

Absorbance measurements allow the calculation of protein concentration in solution via the Beer-Lambert law:

$$A = -\log_{10}(I/I_o) = \epsilon dc$$

Where:
A = absorbance
I = intensity of transmitted light
I_o = intensity of incident light
ϵ = molar extinction coefficient ($M^{-1}cm^{-1}$)
d = cell path length (cm)
c = molar concentration (M)

The calculation requires the knowledge of the appropriate extinction coefficient, which is usually quoted at 280 nm for proteins.

1.2.2 Fluorescence Spectroscopy of Proteins

Fluorescence emission may be observed when an electron returns from the first excited state (S_1) to the ground state (S_o). The emission is invariably shifted to a lower wavelength (Stokes shift) due to the rapid decay to the lowest vibrational level of S_1 prior to emission. Additionally fluorophores generally decay to excited vibrational levels of S_o, producing a further loss in energy.

Solvents can have an effect on fluorescence emission. On excitation a fluorophore becomes an instantaneous dipole (Franck-Condon principle). In polar solvents, the polar excited state will be stabilized, leading to a lowering of the energy gap between S_o and S_1 levels and hence a red shift in emission in comparison with non-polar solvents. This shift to longer wavelength is usually accompanied by a drop in emission intensity due to solvent quenching. Thus, information concerning a fluorophore's environment can be gained from fluorescence studies, which in turn, provides protein structural information.

Proteins possess only three amino acids which are intrinsically fluorescent; tryptophan, tyrosine and phenylalanine. These fluorophores can be excited separately (fig 13), however the emission spectra of proteins containing several of these fluorophores are dominated by tryptophan due to energy transfer from phenylalanine and tyrosine to tryptophan.

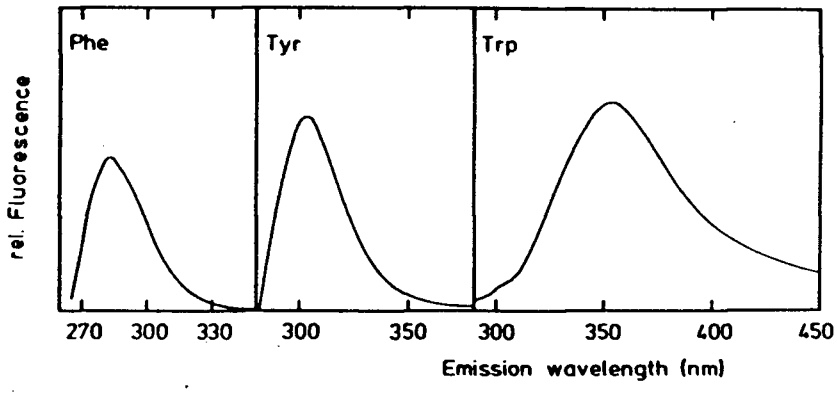

Fig 13: Fluorescence spectra of the aromatic acids in 0.01 M potassium phosphate buffer, pH 7.0, at 25° C. **Phe**, 100 µM phenylalanine excitation 257 nm; **Tyr**, 6 µM tyrosine excitation 274; **Trp**, 1 µM tryptophan excitation 278 nm. Creighton (1989).

A more specific method to study protein structure via fluorescence is to introduce extrinsic fluorophores. Acrylodan (6-acryloyl-2-dimethylaminonaphthalene, fig 14) is a particularly environment-sensitive fluorescent probe which reacts only with cysteine residues (Pendergast et al., 1983) *N*-(1-pyrene)iodoacetamide (fig 15) is another cysteine specific probe which has proved useful in studying actin, as the fluorescence of pyrene-labeled actin is sensitive to polymerization (Cooper et al., 1983).

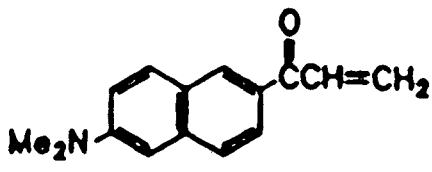

Fig 14: 6-acryloyl-2-dimethylaminonaphthalene

Fig 15: *N*-(1-Pyrene)iodoacetamide

1.2.3 Protein CD Spectroscopy

Optically active substances absorb left and right circularly polarized light (L and R, respectively) to different extents. This difference is usually expressed in terms of extinction coefficients.

$$\epsilon_L - \epsilon_R = \Delta\epsilon$$

Where ϵ_L = extinction coefficient for L ($M^{-1}cm^{-1}$)
ϵ_R = extinction coefficient for R ($M^{-1}cm^{-1}$)
$\Delta\epsilon$ is called the circular dichroism.

As a result of the different absorbances of L and R, the combination of the two waves will produce elliptically polarized light. This fact has led to circular dichroism being expressed in terms of the ellipticity, θ, of the ellipse that characterizes such light, where tan θ is equal to the ratio of the minor axis to the major axis of the ellipse. $\Delta\epsilon$ is related to the molar ellipticity $[\theta]$ by:

$$[\theta] = 3300\,\Delta\epsilon$$

A curve showing the dependence of θ on wavelength is called a CD spectrum. Molar ellipticity, $[\theta]$ in deg cm^2 $dmol^{-1}$, can be calculated from observed ellipticity at a specific wavelength:

$$[\theta] = M\theta / 10dc$$

Where; θ is the observed ellipticity (deg)
M is the molecular mass (g mol^{-1})
d is the cell path length (cm)
c is the concentration (g ml^{-1})

If M expresses the mean residue molecular mass, then [θ] is called the mean residue (or residual) ellipticity.

Protein CD spectra are dominated by the signal from the peptide bond backbone, the various conformations of which have characteristic spectra (fig 16).

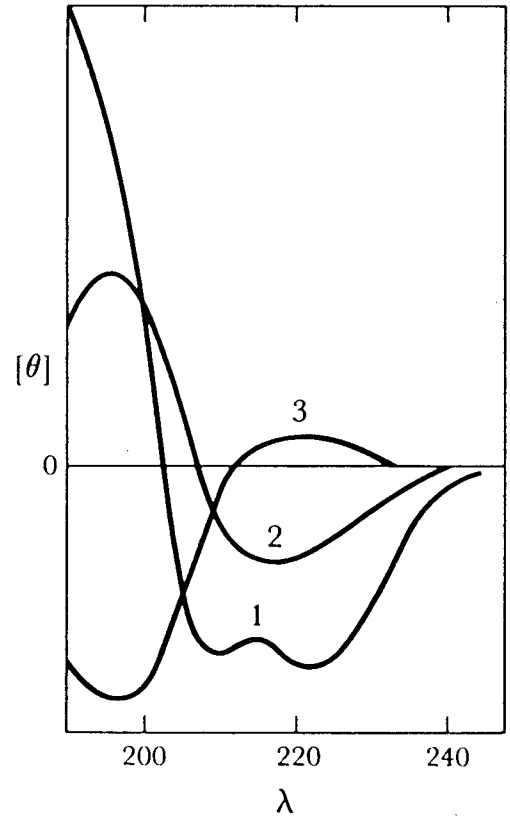

Fig 16: CD spectra of poly-L-lysine in the 1, α-helical; 2, β-sheet; 3, random coil conformations. Freifelder (1976).

Using these standard spectra the percentage α-helix, β-sheet and random coil can be calculated by solving the following equation at two different wavelengths and using the restraint, $f_H + f_B + f_R = 1$.

$$[\theta] = f_H X_H + f_B X_B + f_R X_R$$

Where: $[\theta]$ = mean residue ellipticity (deg cm^2 $dmol^{-1}$)

f = fraction of amino acid residues in each of the following conformations: H, α-helix; B, β-sheet and R, random coil (or more properly undefined structure).

X_H, X_B, X_R are the mean residue ellipticities of 100% α-helical proteins, 100% β-sheet proteins and 100% random coil proteins respectively

CD also provides a good method for studying the stability of proteins. The loss of CD signal between 210 nm and 230 nm on denaturation (thermal or chemical) is due to loss of protein structure. The α-helix and β-sheet structures unfold into the random coil structure, which has relatively low CD. By monitoring this loss of signal the stability of a protein can be assessed.

2: Materials and Methods

Part 1: Proteins

2.1.1 The Preparation of G-Actin

The preparation of G-actin from rabbit muscle powder was based on the method of Spudich and Watt (1971). Acetone powder (10 g) was extracted with buffer A (200 ml, 2 mM Tris-HCl, 0.2 mM $CaCl_2$, 0.2 mM ATP, 1.0 mM DTT, pH 7.6) for 30 min on ice. The solution was filtered through a double layer of cheesecloth, and then through preparative grade filter paper. The residue was rewashed (100 ml, buffer A) and refiltered, the solid residue was discarded. The filtrates were combined, centrifuged (40,000 rpm, Beckman 45Ti rotor, 1 h, 4 °C,) and KCl (to 50 mM) and $MgCl_2$ (to 2 mM) were added to the supernatant. The crude actin was allowed to polymerize at room temperature for 2 h, at which point solid KCl was added to 0.8 M with gentle stirring (1.5 h). The solution was centrifuged (40,000 rpm, Beckman 45Ti rotor, 3 h, 4 °C) and the pellet (F-actin) resuspended in 30 ml of buffer A and dialysed (64 h against 3 changes, each of 1 L of buffer A, 4 °C). The solution was centrifuged (40,000 rpm, Beckman 45Ti rotor, 3 h, 4 °C) and the supernatant, G-actin, was used immediately or dialysed against buffer A.

2.1.2 Preparation of Pyrene-actin

Pyrene-actin was prepared by a modified version of the method proposed by Cooper et al., 1983. PIA (6 mg, Molecular Probes Inc., Eugene, OR) was dissolved in 1 ml of DMF/acetone (2:1). This solution then was shaken (20 h, room temp.) with 3 ml of actin (1 mg/ml) which had previously been polymerized (2 mM $MgCl_2$, 50 mM $CaCl_2$, 2 h, room temp.). The product then was dialysed against 1L buffer A (3 changes each of 12 h, 4 °C) and centrifuged (40,000 rpm, Beckman 45Ti rotor, 3h, 4 °C). The supernatant, pyrene-actin, was stored in buffer A.

2.1.3 Acrylodan-actin Preparation

Actin was labeled with the fluorescent reagent acrylodan following the method of Marriott et al. (1988). G-actin (1 ml of a 1 mg/ml solution in buffer A) was dialysed for 12 h at 4 °C against 2 mM Tris-HCl, 0.2 mM ATP, 0.1 mM $CaCl_2$, pH 7.9. The G-actin was polymerized to F-actin by the addition of $MgCl_2$ to 2 mM for 2 hours at room temperature. An excess of acrylodan (5×10^{-5} M final concentration, Molecular Probes Inc., Eugene, OR) dissolved in a minimum of DMF (~ 0.2 ml) was added directly to the F-actin. The mixture was rocked in the dark (6 h) at room temperature. The resulting acrylodan-labeled F-actin was dialysed against buffer A (1L, 3 changes in 60 h, 4 °C) in the dark before being centrifuged (40,000 rpm, Beckman Type 50 rotor, 3 h, 4 °C) to produce acrylodan-labeled G-actin (acrylodan-actin) in the supernatant.

2.1.4 The Acrylodan-actin Assay

The following acrylodan-actin assay is a modification of that first used by Safer (1989) to test for DBP and other actin-binding proteins in mixed protein solutions. The assay utilizes the fact that DBP is one of two proteins, in plasma, that can bind specifically to actin.

Acrylodan-actin (10 µl of a 1 mg/ml solution in buffer A) was combined with each of the samples to be tested (10 µl), along with a crystal of analytical grade sucrose which was included to facilitate loading into the sample wells of the electrophoretic gel. These then were loaded onto a non-denaturing polyacrylamide electrophoretic gel [6 ml buffer E (25 mM Tris-HCl, 194 mM glycine, 0.2 mM ATP), 7.5% acrylamide, 0.2% N,N'-methylenebisacrylamide, 70 µl of freshly prepared ammonium persulphate (0.1 g/ml), 10 µl Triton-X 100, 10 µl TEMED, pH 8.4] which was run on a Mini-Protean II system (Bio-Rad Labs, Richmond, CA) in buffer E at 200 volts for 45 min. When veiwed under a UV light the positive samples revealed a slow moving band due to the DBP-actin complex in addition to the band corresponding to uncomplexed acrylodan-labeled G-actin.

2.1.5 The Collection of Horse Plasma

The method of collecting plasma was based on the procedure Côté and Smillie (1981) employed to prepare platelets. Blood (120 L) from freshly slaughtered horses (Alsask Processors, Edmonton) was collected, with frequent stirring, into three plastic 50 L pails, each containing 9 L of anticoagulant (720 g sodium citrate, 89 g citric acid, 61 g sodium dihydrogen orthophosphate, 1400 g dextrose dissolved to 27 L in water). Protease inhibitors, pepstatin, leupeptin (12.5 mg of each per 50 L bucket, Sigma, St. Louis, MO) and PMSF (0.2 mM), were added.

The blood was allowed to stand (~1 h) until two distinct layers had formed, with a platelet-rich upper layer and a red cell-rich lower layer. Plasma was collected as the supernatant of a 5,000 rpm centrifugation (Sorvall RC-3 rotor, 15 min at 4 °C) of the platelet-rich layer. It was frozen in 500 ml to 2 L portions and stored at -20 °C.

2.1.6 The Purification of DBP

Equine DBP was prepared using a modified version of the method proposed by Chapuis-Cellier et al. (1982) to purify human DBP. Pepstatin (100 µl of a 2 mg/ml stock solution in DMSO; Sigma, St. Louis, MO) and Leupeptin (100 µl of a 2 mg/ml stock solution in water; Sigma, St. Louis, MO) were added to thawed horse plasma (80 ml). The plasma was dialysed (12 h, 30 mM sodium phosphate buffer, 0.1%(w/v) sodium azide, 50 µM PMSF, pH 7.0, 4 °C) and centrifuged at 18,000 rpm for

30 min (Sorvall SS34 rotor). The pellet was discarded and the supernatant was applied (1 ml/min), at room temperature, to an Affi-Gel Blue affinity chromatography column (2.5 x 100 cm, 50-100 mesh, Bio-Rad Laboratories, Richmond, CA) in buffer B (30 mM sodium phosphate, 0.1%(w/v) sodium azide, pH 7.0). The elution of protein was followed by UV absorbance at 280 nm, and the region where DBP eluted was determined using the acrylodan-actin assay (also employed to follow DBP through subsequent chromatographic columns). The Affi-Gel Blue column removed the major plasma protein, albumin, as well as providing some fractionation of other plasma proteins (Gianazza et al., 1982). The column was regenerated by applying 2 L of potassium thiocyanate (1.5 M) in the running buffer, as recommended by the manufacturer.

The active fractions were pooled (~250 ml) and concentrated to about 20 ml by ultrafiltration using a YM30 membrane (Amicon, Danvers, MA) and then applied (1 ml/min), at room temperature, to a Bio-Gel P100 gel filtration column (5 x 110 cm, Bio-Rad Labs, Richmond, CA) in buffer B. The active fractions of the eluate then were applied (0.5 ml/min) directly to a hydroxylapatite column (2.0 x 20 cm, Bio-Rad Labs, Richmond, CA) again in buffer B at room temperature. A 30 to 100 mM phosphate gradient in buffer B was used to elute the bound protein. 5 ml fractions were collected.

A Flow Chart Showing the Purification of DBP

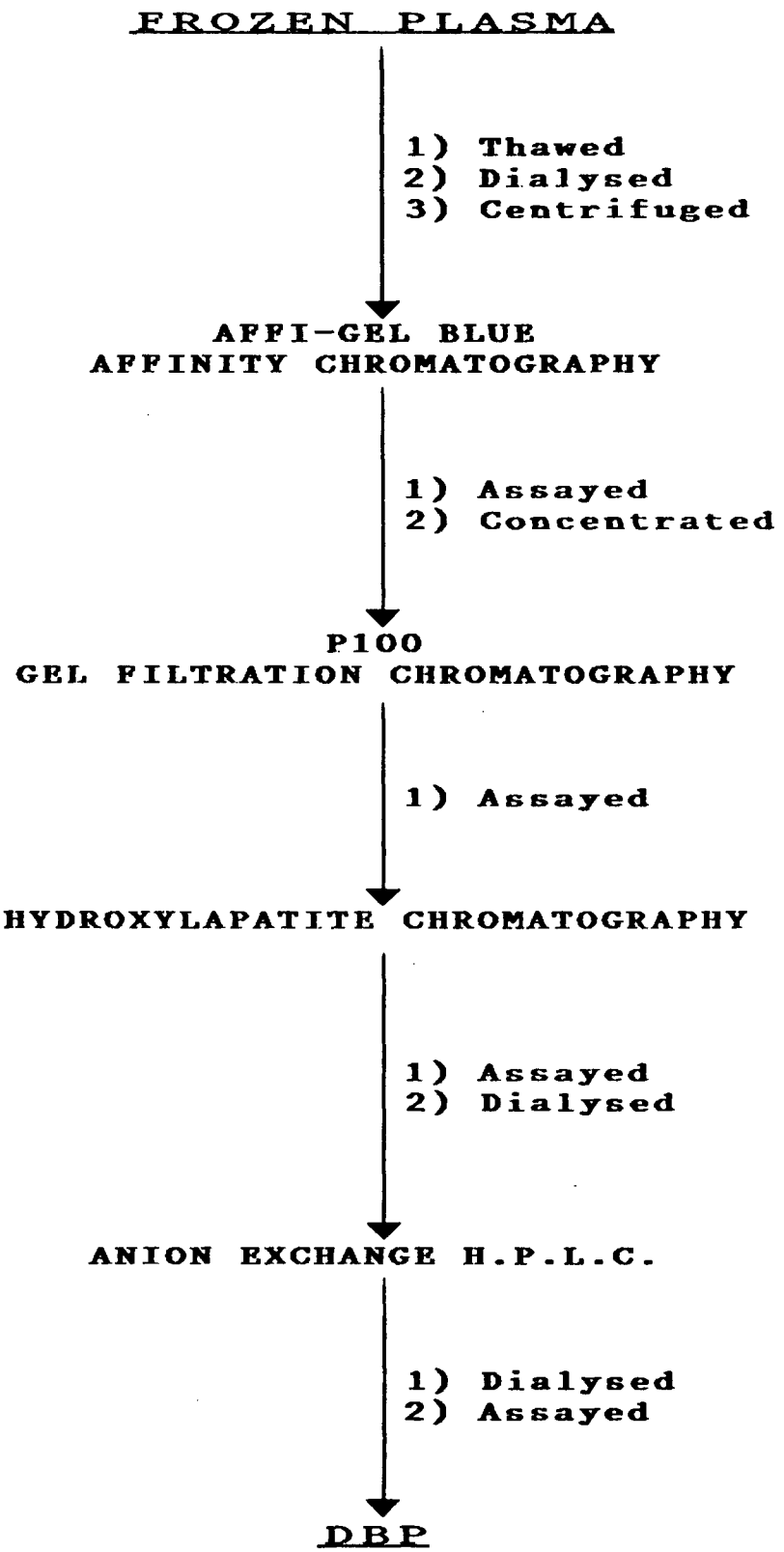

The active fractions were dialysed (12 h, 10 L buffer B, 4 °C) and filtered (0.22 μM Millipore filter). Small volumes (2 ml) were applied, at room temperature, to a HPLC anion exchange column (200 x 4.6 mm, Aquapore AX-300, 7 micron pore size, Brownlee Labs, Santa Clara, CA). DBP was eluted as a single peak with a salt gradient (0-0.25 M NaCl in buffer B).

2.1.7 Calculation of an Extinction Coefficient for DBP

Using the approximation that the molar extinction coefficient of DBP will be equal to that of the denatured protein and the fact that tyrosine, tryptophan and cysteine are the only absorbing species in the 276-282 nm wavelength range, the following estimation of molar extinction coefficient at 280 nm can be made (Gill and von Hippel, 1989):

$$\epsilon = a\epsilon_{Tyr} + b\epsilon_{Trp} + c\epsilon_{Cys}$$

Where: ϵ_{Tyr}, ϵ_{Trp} and ϵ_{Cys} are the molar extinction coefficients at 280 nm and a, b and c are the number of each type of amino acid per protein molecule.

2.1.8 Preparation of Acrylodan-DBP

DBP (2 ml of a 1 mg/ml solution in 20 mM MOPS, 0.1% NaN_3, pH 7.3) was shaken for 12 hours at room temperature with acrylodan (5×10^{-5} M, Molecular Probes Inc., Eugene, OR) dissolved in a minimum of DMF (~0.2 ml). The product was dialysed extensively against 20 mM MOPS, 0.1% NaN_3, pH 7.3 (4 changes each of 1 L for 12 h at 4 °C) before being centrifuged (40,000 rpm, Beckman Type 50 rotor, 1 h, 4 °C). The pellet was discarded.

2.1.9 Gel Electrophoresis

Gel electrophoresis was carried out using one of the following electrophoretic systems: Mini-Protean II system (Bio-Rad Labs, Richmond, CA) or PhastSystem (Pharmacia, Uppsala, Sweden). The PhastSystem was generously made available by Dr. Dana Devine.

Part 2: Spectroscopic Methods

2.2.1 Absorbance Spectra

Absorbance measurements and second derivative absorbance spectra were performed on a Lambda 4B UV/VIS Spectrophotometer (Perkin Elmer, Norwalk, CT).

2.2.2 Fluorescence Spectra

Fluorescence spectra were recorded on a LS-5B Luminescence Spectrometer in conjunction with a 7500 Professional Computer (Perkin Elmer, Norwalk, CT). The spectrometer was equipped with a thermostated circulating water bath (Haake, Berlin, Germany), and a temperature equilibration period of 15 min was allowed before each measurement.

2.2.3 CD Spectra

CD spectra were generated on a rebuilt J-20 Automatic Recording Spectro-Polarimeter (Jasco, Tokyo) which was equipped with a temperature controlled, nitrogen purged sample chamber. All samples were allowed to equilibrate in the chamber for 15 min before measurements were taken. The output was standardized using D-Pantolactone (12 mg in 100 ml of H_2O) which has an ellipticity of -17.3×10^3 deg cm^2 $dmol^{-1}$ at 220 nm (Tuzimura et al., 1977).

3: Results and Discussion

3.1.1 Yield and Purity of DBP

DBP was eluted in a single peak (fig 17) from the HPLC column in the final stage of the purification scheme. A total of 6-7 mg of DBP were retrieved per 80 ml of starting plasma, affording a yield of 21-25%, assuming an initial plasma concentration of 350 mg/L (Bouillon et al., 1986). The purification scheme was reproducible, yielding DBP from six runs in succession.

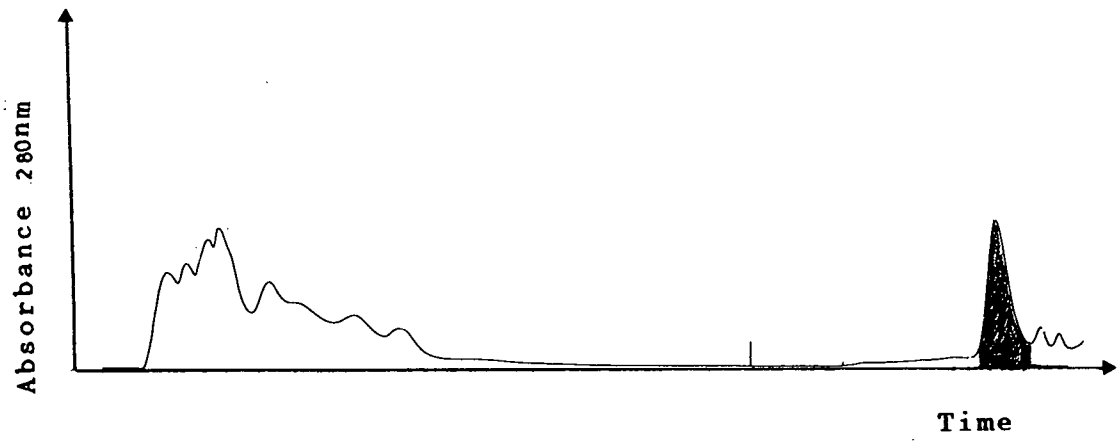

Fig 17: Elution profile from HPLC column. Shaded area corresponds to DBP.

The peak contained a single protein that migrated as a solitary band on a SDS-polyacrylamide electrophoretic gel

under reducing conditions (fig 18). DBP also migrated as a single band when subjected to non-denaturing, non-reducing polyacrylamide gel electrophoresis. Furthermore, on non-reducing SDS-polyacrylamide electrophoretic gels monomeric DBP constituted the major species present (>95%), with only a very faint band due to DBP dimers (Bouillon et al., 1977).

Fig 18: SDS polyacrylamide electrophoretic gel. Lanes from left to right: 1, Plasma; 2, Affi-gel blue eluate; 3, P 100 eluate; 4, Hydroxylapatite eluate; and 5, HPLC eluate.

3.1.2 Optical Spectra

The absorbance spectrum of DBP revealed a typical tryptophan-free profile (fig 19a). The peak at 277 nm and shoulder at 284 nm are features of tyrosine absorbance and the undulations between 255 and 275 nm are indicative of the underlying phenylalanine spectrum. If tryptophan had been present a shoulder at 290 nm would have been expected and the absorbance maximum would have been nearer 280 nm, as for albumin (fig 19b).

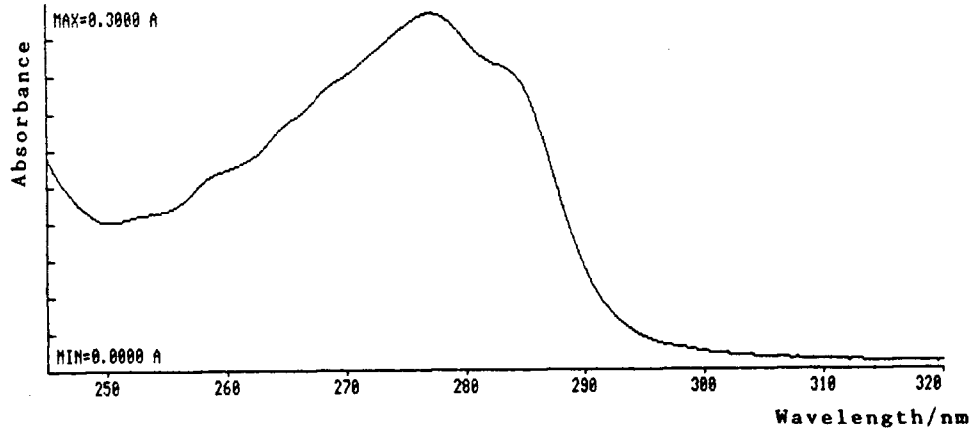

Fig 19a: Absorbance spectrum of DBP (0.7 mg/ml).

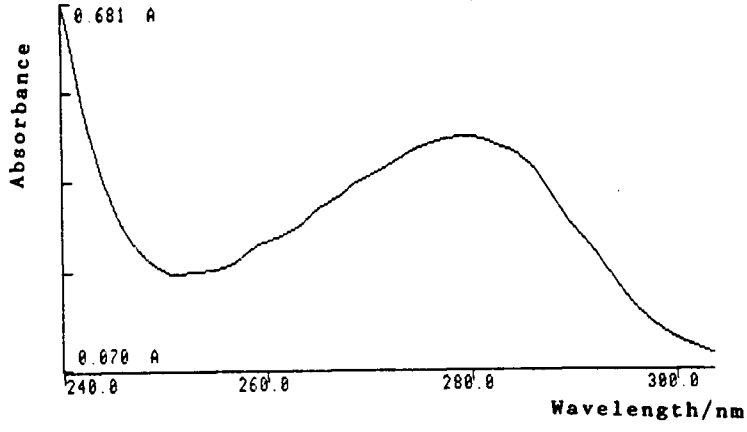

Fig 19b: Absorbance spectrum of albumin (0.7 mg/ml).

An extinction coefficient of 22,560 M^{-1} cm^{-1} was calculated for DBP from the reported sequence of rat DBP (Cooke, 1986).

The second derivative absorbance spectrum shows more clearly the lack of tryptophan. Proteins containing tryptophan have a negative peak at 290 nm, here a positive peak at 290 nm is seen (fig 20). This peak is characteristic of tyrosine. Furthermore the spectrum resembles the superposition of tyrosine and phenylalanine second derivative spectra (page 16).

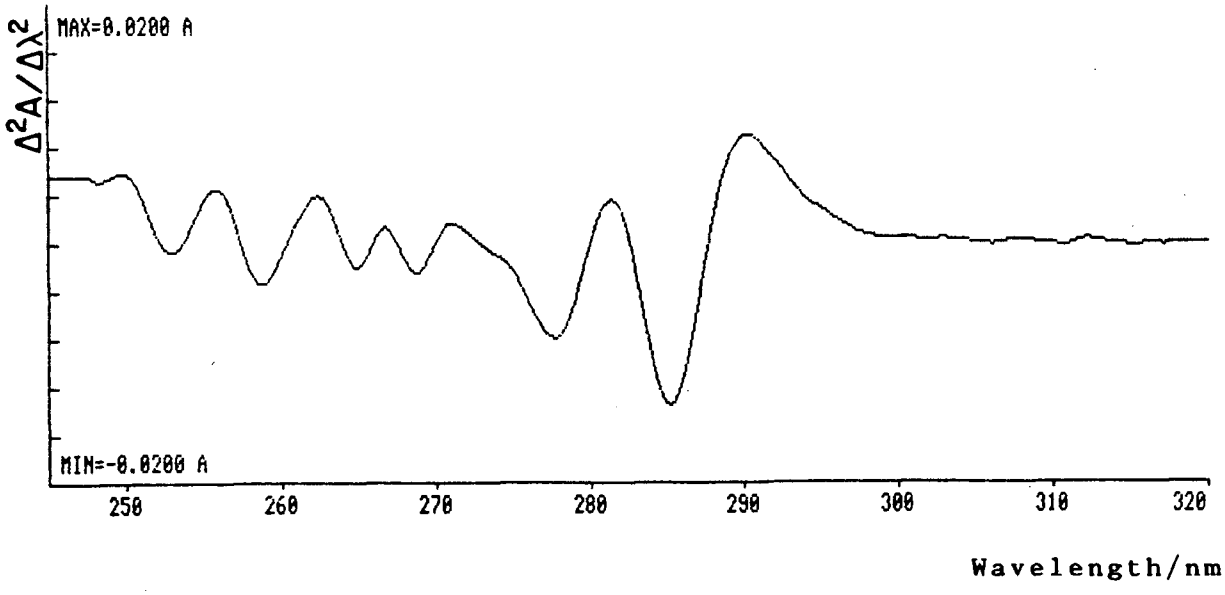

Fig 20: Second derivative absorbance spectrum of DBP (0.7 mg/ml).

The fluorescence emission spectrum, excitation at 278 nm, is again typical of a protein containing tyrosine and no tryptophan (fig 21). The maximum at 307 nm is that characteristic of tyrosine, and the fluorescence intensity is low around 330-350 nm where tryptophan fluorescence peaks.

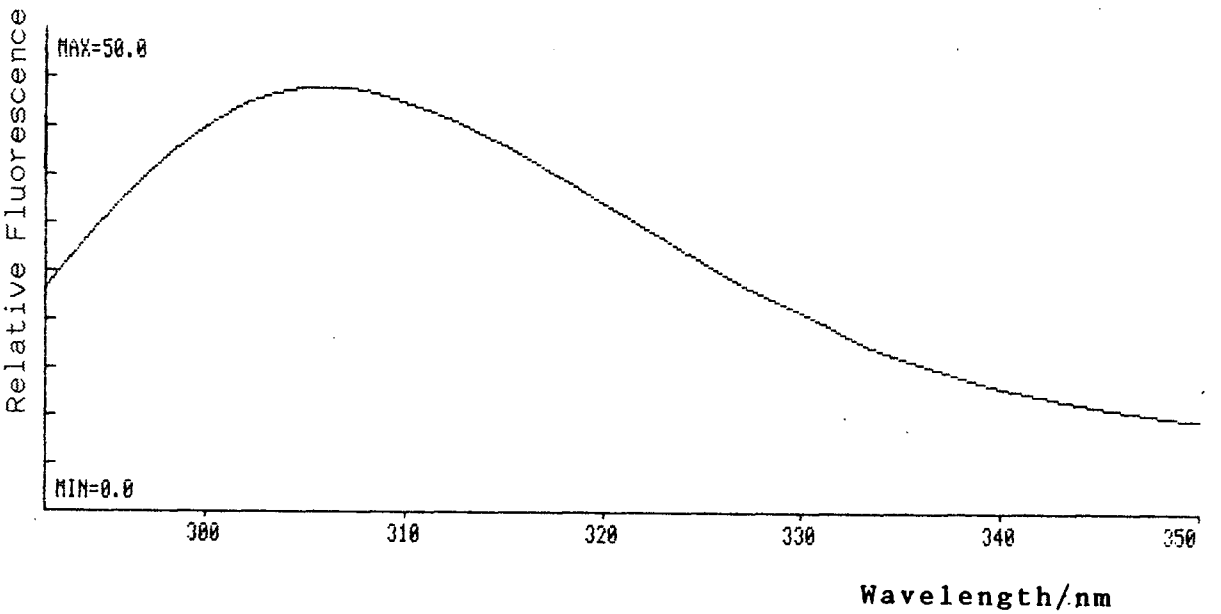

Fig 21: Fluorescence emission spectrum, excitation 278 nm, of DBP (0.7 mg/ml) at 20 °C.

These three optical spectra all show that the isolated protein does not contain tryptophan but does have tyrosine and phenylalanine. This is consistent with the reported amino acid sequence for rat plasma DBP (Cooke, 1986).

3.1.3 Actin assays

Evidence of DBP's actin-binding properties was gained from the assay used to isolate the protein (page 25). Acrylodan-actin moves as a single band on non-denaturing electrophoretic polyacrylamide gels, but in the presence of DBP, a second, slower moving band is seen due to the formation of DBP-acrylodan-actin complex (fig 22).

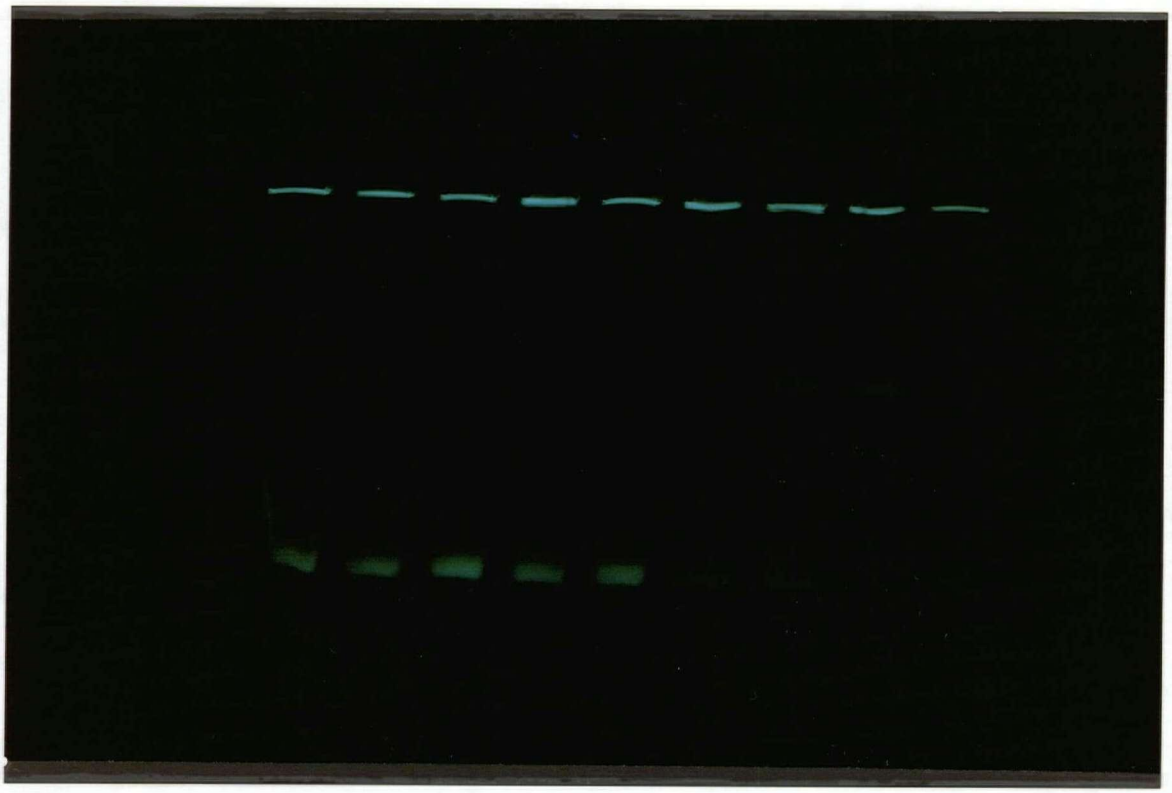

Fig 22: The acrylodan-actin assay of Affi-gel Blue fractions. Lanes from left to right see band appearing in centre of gel due to DBP-acrylodan-actin complex. Lower band = G-actin, upper band = F-actin that did not enter the gel.

Further evidence for the actin-binding activity of DBP arises from pyrene-actin fluorescence studies. The fluorescence intensity at 386 nm on excitation at 344 nm greatly increases on polymerization of pyrene-G-actin to pyrene-F-actin (fig 23a). In the presence of DBP this increase does not occur (fig 23b). DBP sequesters actin monomers preventing polymerization. The addition of DBP to pyrene-F-actin results in a slow fall in fluorescence (fig 23c). This is due to DBP tying up the free pyrene-G-actin, thus shifting the equilibrium away from the polymerized state, resulting in a slow depolymerization, returning to a G-pyrene-actin fluorescence level after 10 hours. This effect is characteristic of an actin monomer-binding protein.

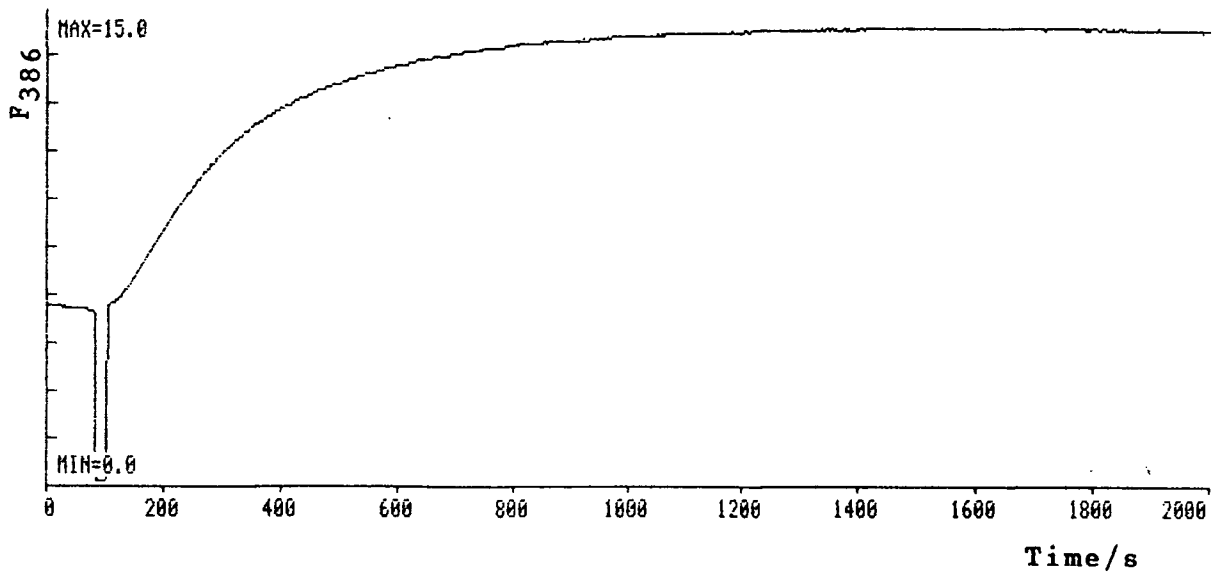

Figure 23: Time related pyrene-actin fluorescence studies, excitation at 344 nm and emission at 386 nm at 20 °C.

a) G-actin (0.2 mg), pyrene-G-actin (0.02 mg) in buffer A (1 ml total). 2 µl of $MgCl_2$ (1 M) added after 80 s.

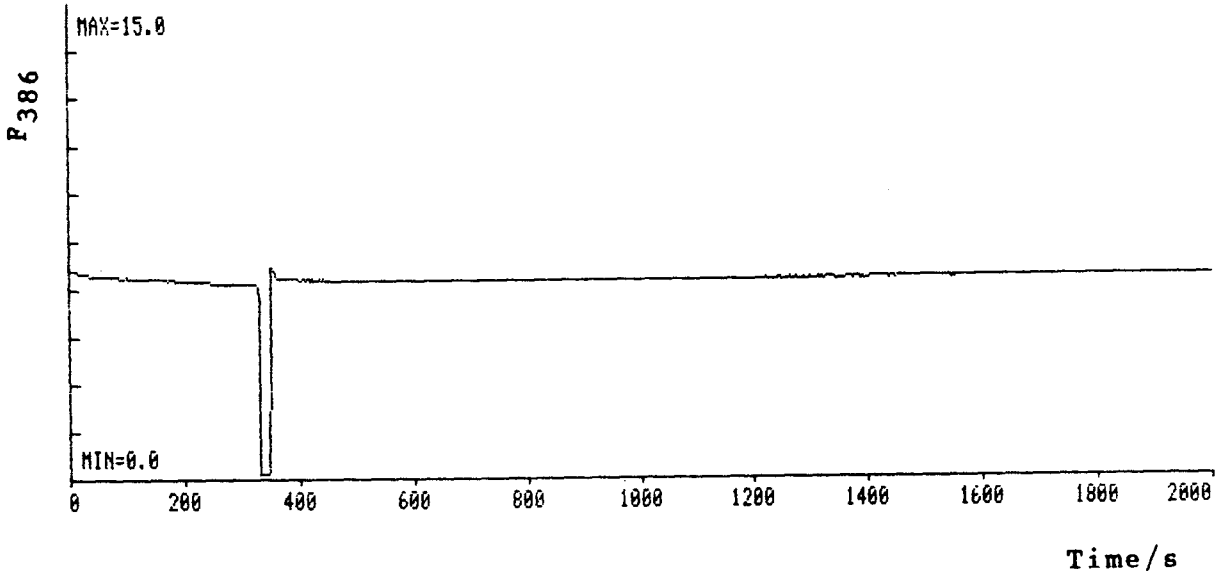

b) G-actin (0.2 mg), pyrene-G-actin (0.02 mg), DBP (0.27 mg) in buffer A (1 ml total). (1:1 ratio of actin to DBP). 2 µl of $MgCl_2$ (1 M) added after 340 s.

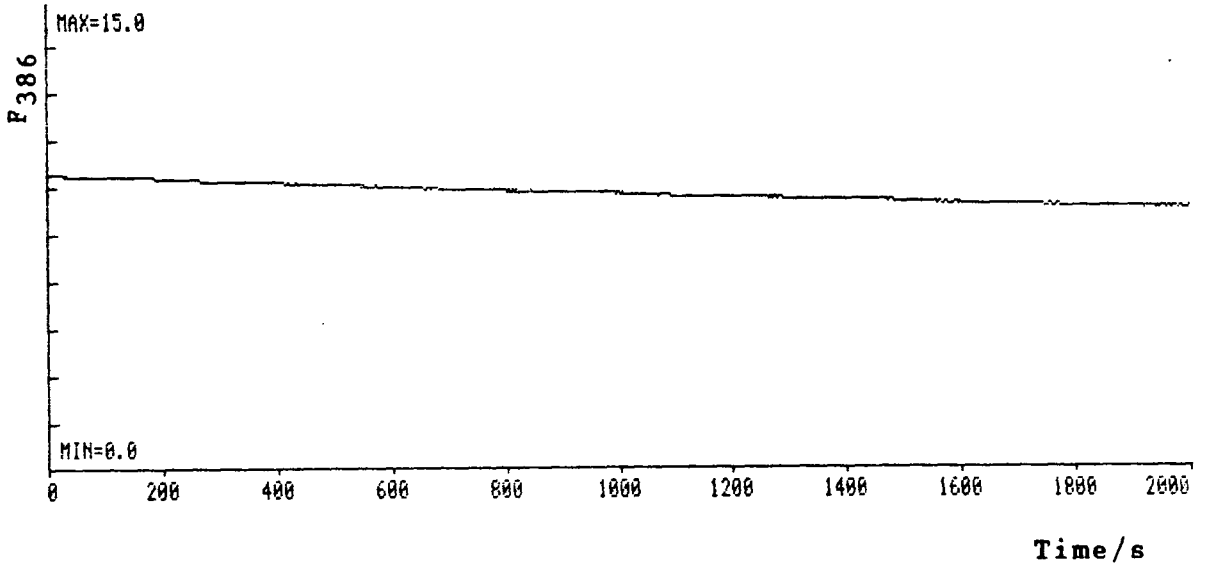

c) G-actin (0.15 mg), Pyrene-G-actin (0.015 mg) incubated , 0.5 h, with 2 mM $MgCl_2$. At t = 0 DBP (0.2 mg) added, final volume 1 ml.

3.1.4 Calculation of Molecular Mass

DBP and molecular mass standards were run on a denaturing SDS electrophoretic gel (fig 24). From the relative distance moved by DBP in comparison to the standards, a molecular mass of 53,000 ± 3,000 was calculated (fig 25).

Fig 24: SDS polyacrylamide electrophoretic gel. Lanes 1 and 3 top to bottom molecular mass standards: 95,000; 55,000; 43,000; 36,000; 29,000; 18,400; and 12,400. Lane 2, DBP.

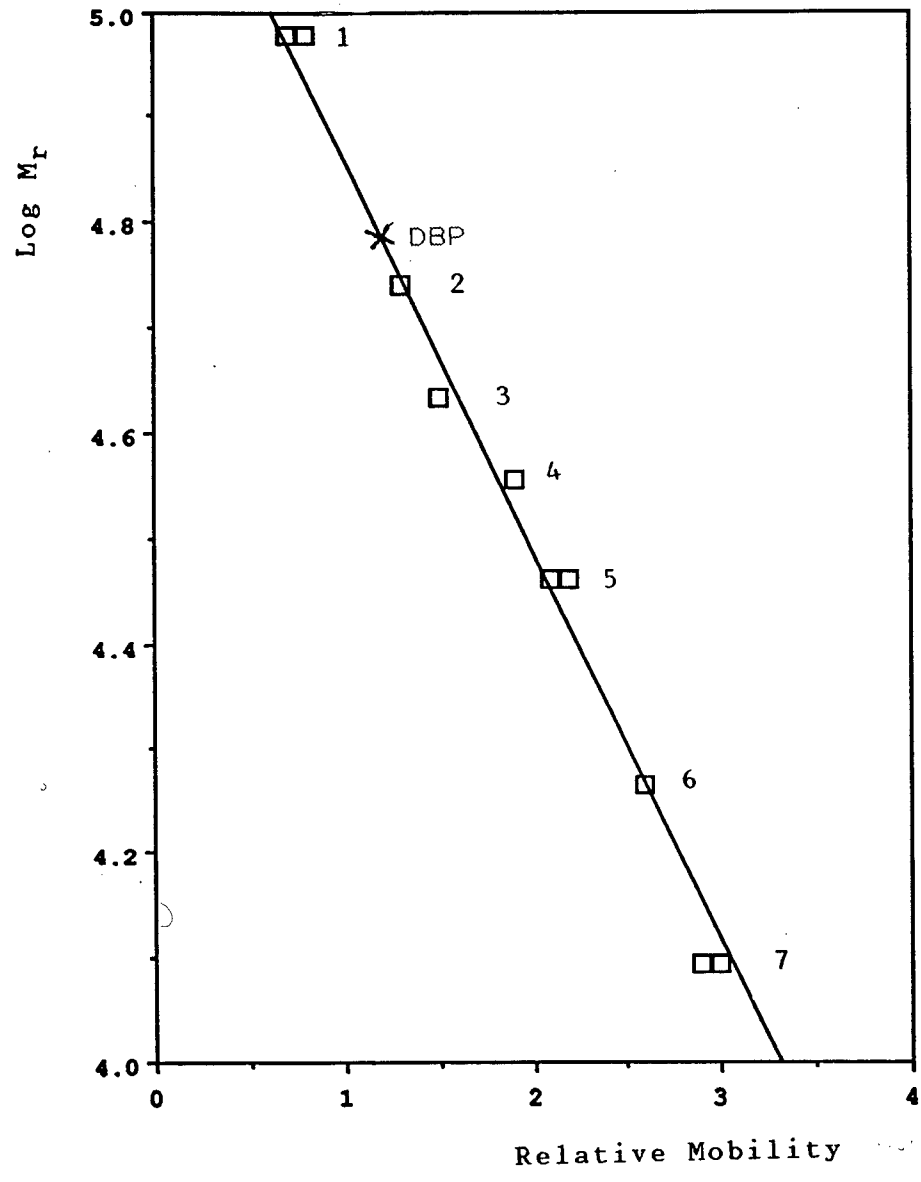

Fig 25: Graph showing the log of molecular mass against distance moved on electrophoretic gel, from the results of 2 runs. 1 = 95,000, 2 = 55,000, 3 = 43,000, 4 = 36,000, 5 = 29,000, 6 = 18,400, and 7 = 12,400 (Pharmacia).

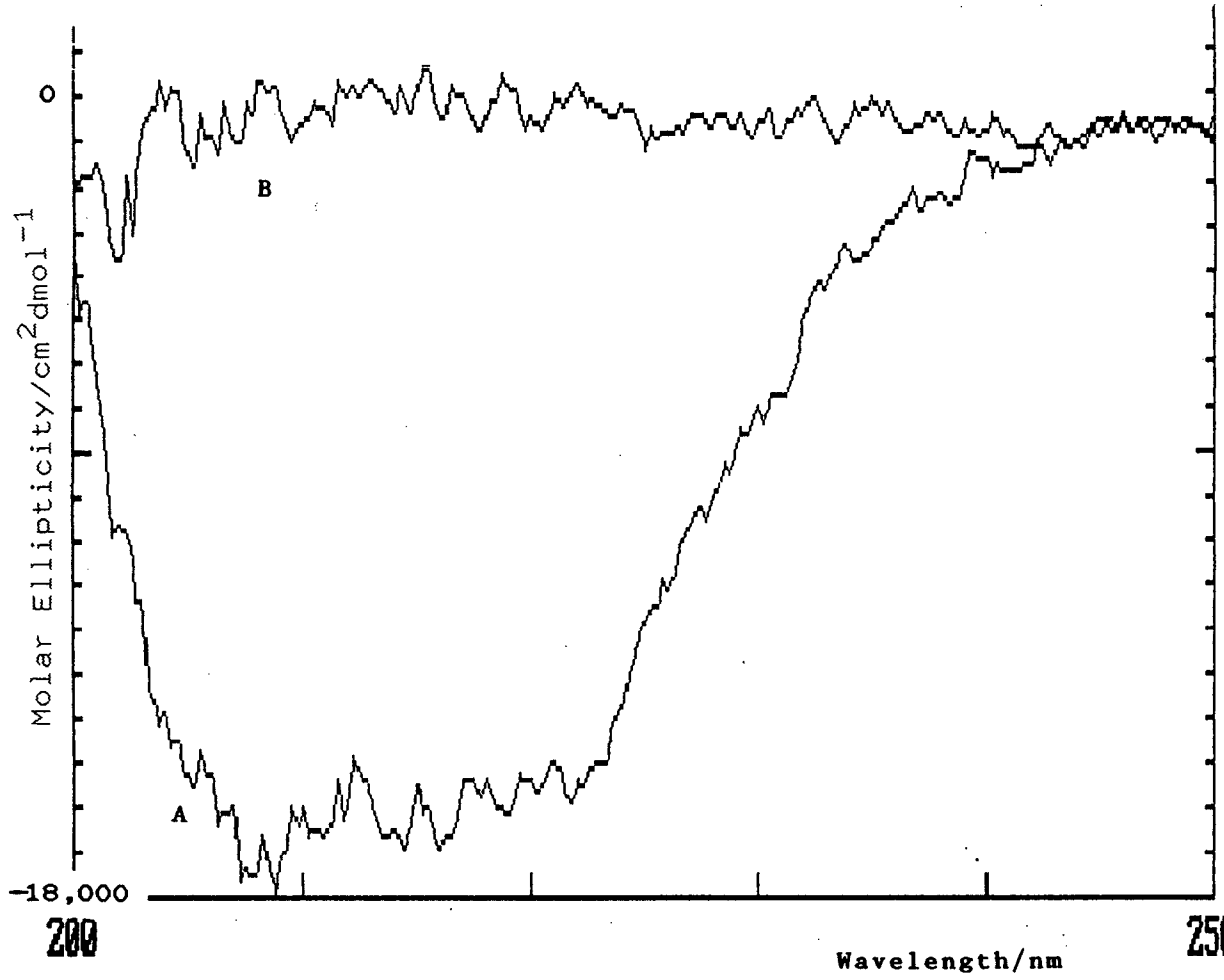

Fig 26: CD spectrum of DBP in 20 mM MOPS, 1 mM EGTA, pH 7.3 at 25 °C.
A) DBP, B) buffer.

3.1.5 Calculation of Secondary Structure

The CD spectrum of DBP (fig 26) is characteristic of a protein high in α-helix and β-sheet structure. Values for α-helix (39%), β-sheet (42%) and random coil (19%) were calculated using X_H, X_B and X_R factors at 225 and 210 nm (Chen et al., 1972).

3.2.1 Thermal Denaturation of DBP followed by CD

The thermal denaturation of DBP in high salt buffer H (150 mM KCl, 20 mM MOPS, 1 mM EGTA, pH 7.3) was followed by CD at 220 nm (fig 27, open squares). DBP was seen to be very stable up to 55 °C, after which the protein started to unfold at a greater rate. However, even at 70 °C a great deal of its structure was retained. On cooling to 15 °C the signal returned to 97% of its original value, suggesting that the molecule was able to refold. This recooled DBP was shown to retain actin-binding activity using the acrylodan-actin assay.

A second sample, which had been incubated at room temperature with 5 mM DTT (2 h) and then dialysed at 4 °C against buffer H + 2 mM DTT (12 h), also was subjected to thermal denaturation (fig 27, closed triangles). DTT has the effect of breaking disulphide bonds. Here, the initial CD spectrum was indistinguishable from that of the DBP sample without DTT, but on heating, the protein was seen to be much less stable, loosing more CD signal by 40 °C than had the DBP sample without DTT by 70 °C.

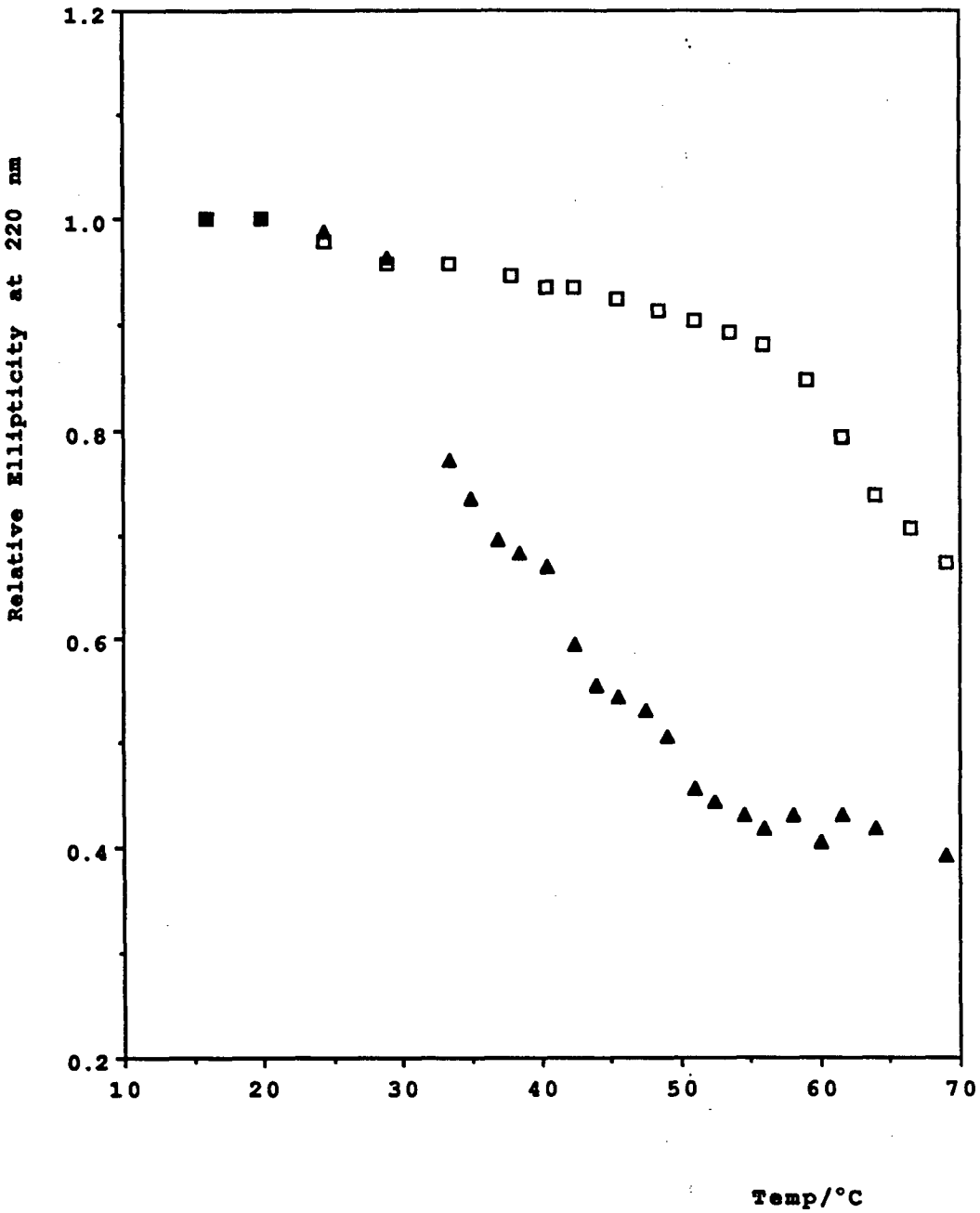

Fig 27: Melting curve of DBP, at high ionic strength, followed by CD at 220 nm.
Open boxes, DBP; closed triangles, DBP + DTT.
Relative ellipticity = θ/(θ at 16 °C).

The recooled sample did not bind actin and only returned to 63% of the original CD signal, suggesting that it did not refold correctly. The disulphide bonds in DBP appear, on this evidence, to be responsible for the unusual stability of this protein, as well as playing a role in the correct refolding of partially denatured DBP. Furthermore, at body temperature (37 °C) the DBP sample which had been incubated with DTT was significantly unfolded, raising the possibility that DBP requires the disulphide bonds to maintain its shape and possibly, to complete its functions.

A similar experiment was carried out in a low salt buffer, buffer L (20 mM MOPS, 1 mM EGTA, pH 7.3) ± DTT (fig 28). The initial CD spectra were similar to those in buffer H, and similar patterns of thermal denaturation were observed. The DBP sample without DTT was again relatively stable up to 55 °C beyond which CD signal was lost at a greater rate. On cooling it retained its actin-binding properties and returned to 92% of the original CD signal.

The sample incubated with DTT was found to be much less stable, as in the high salt case, with the CD signal falling rapidly beyond 30 °C and reaching a value of ~40% at 70 °C, close to that of the high salt + DTT sample. The low salt + DTT DBP sample did not bind actin on cooling and its ellipticity at 220 nm returned to 65% of its original value. These two CD thermal denaturation experiments suggest that the disulphide bonds play a major role in stabilizing DBP and that ionic strength does not greatly affect stability.

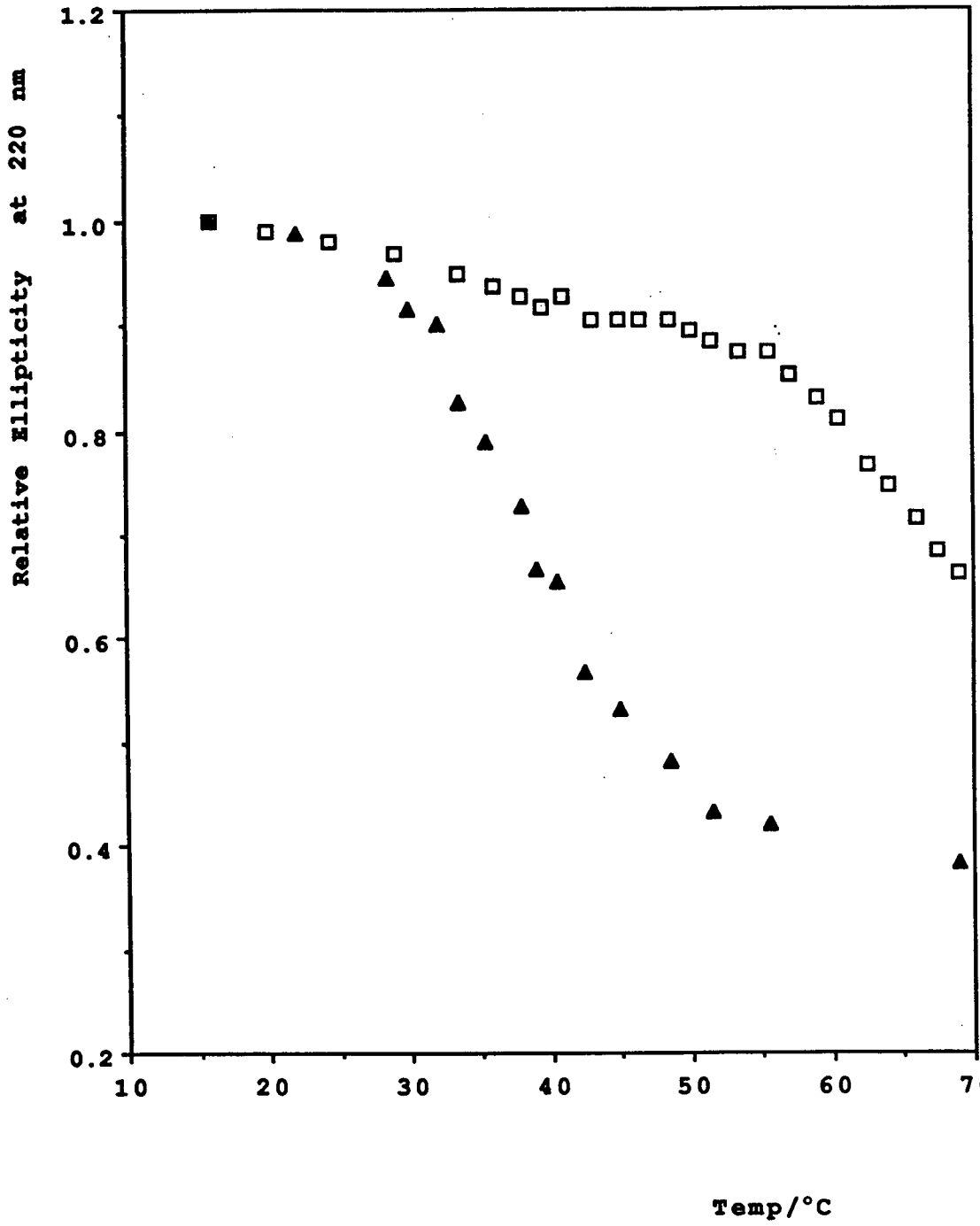

Fig 28: Melting curve of DBP, at low ionic strength, followed by CD at 220 nm.
Open boxes, DBP; closed triangles, DBP + DTT.
Relative ellipticity = θ/(θ at 16 °C).

3.2.2 Thermal Denaturation of DBP Followed by Fluorescence

A further experiment revealing the stabilizing effect of the disulphide bonds against thermal denaturation was carried out by monitoring the effect of temperature on tyrosine fluorescence intensity (fig 29). As proteins unfold, tyrosines generally become more exposed to the solvent, lowering their fluorescence intensity. This effect is superimposed over the inherent temperature dependence of fluorescence. The DBP sample which had been incubated with DTT lost fluorescence intensity at 307 nm, excitation at 278 nm, more rapidly with temperature than the non-reduced DBP sample. The reduced DBP did not have the structural stabilization provided by the disulphide bonds, and unfolded at a lower temperature. On recooling the DBP sample without DTT returned to 95% of its original fluorescence compared to 62% for the sample with DTT, consistent with the CD data, and indicating that the DBP without disulphide bonds was unable to refold.

3.2.3 Guanidine.HCl Induced Denaturation Followed by CD

The denaturation of DBP by guanidine hydrochloride in buffer H ± DTT was followed by CD at 220 nm (fig 30). The experiment did not reveal a significant difference between the unfolding patterns of the DBP samples with or without DTT. The CD signal fell sharply between 1 and 2.5 M guanidine hydrochloride reaching a value of about 10% at 4 M GuHCl.

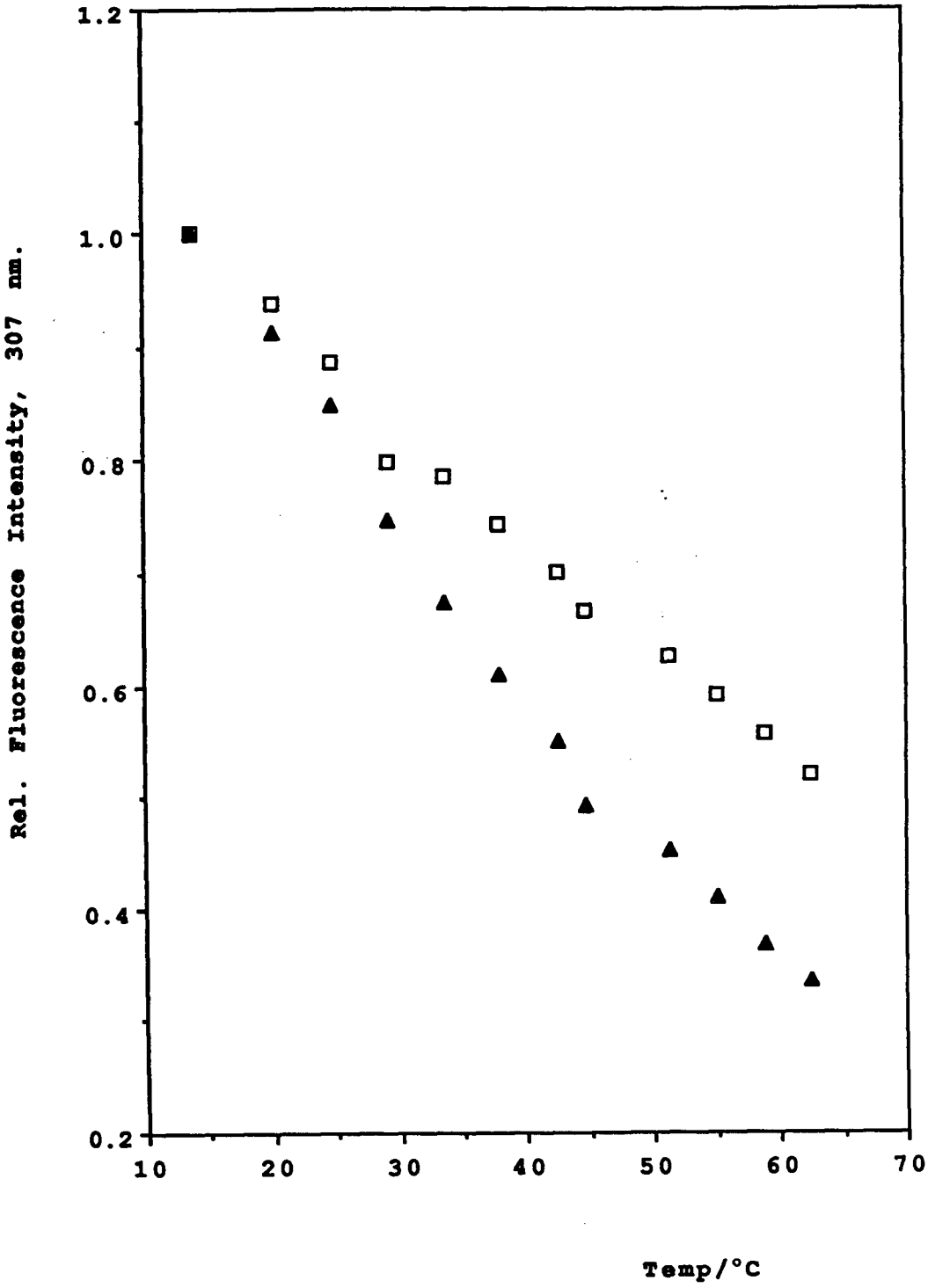

Fig 29: Melting curve of DBP followed by fluorescence emission at 307 nm, excitation at 278 nm. Open boxes, DBP; closed triangles, DBP + DTT. Relative fluorescence = F/(F at 14 °C).

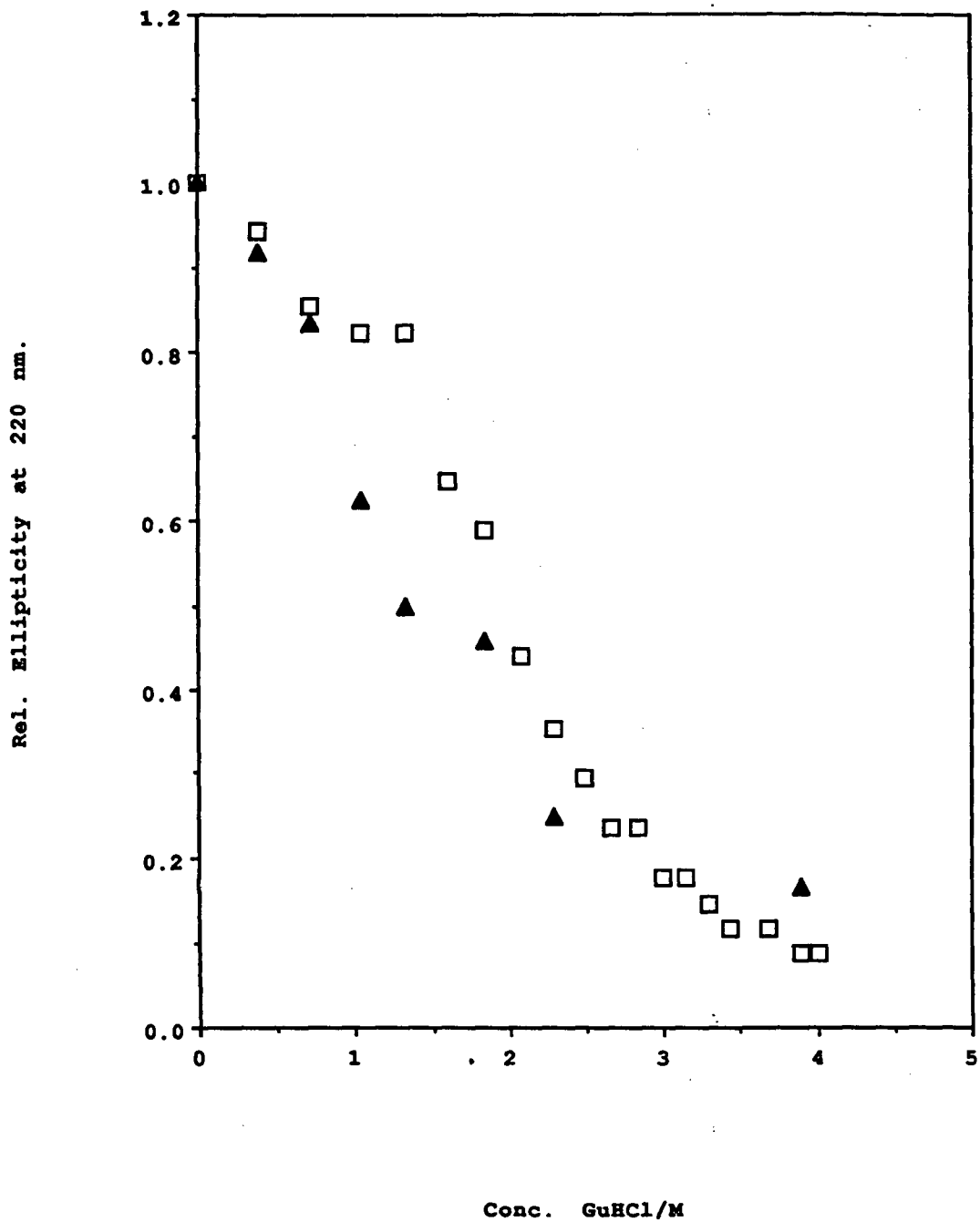

Fig 30: Guanidine Denaturation of DBP followed by CD.
Open boxes, DBP; closed triangles, DBP + DTT.
Relative ellipticity = θ/(θ at 14 °C).

In comparison to the thermal melting curves of DBP in the presence of DTT ± salt (figs 27 + 28), the guanidine denaturation proceeds to a farther point than thermal denaturation. Indeed at 70 °C the thermally denatured DBP samples with DTT appear to be reaching a plateau at around 38% of original signal. This may be due to the protein reaching a relatively stable, partially-unfolded state (molten globular state) (Kuwajima, 1989).

3.3.1 Acrylodan Labeling of DBP

Using the Bio-Rad Protein Assay (Bio-Rad, Richmond, CA) and an extinction coefficient for acrylodan of 129,000 M^{-1} cm^{-1} at 365 nm (Lehrer and Ishii, 1988), the incorporation of the fluorescent label was shown to be 5.0 ± 0.2 acrylodans per DBP. The fluorescence emission and excitation spectra are shown in figure 31.

This degree of labeling was somewhat surprising as Kawakami and Goodman, 1981, found only one relatively inaccessible monothiol group per molecule of human DBP. Furthermore, DBP is known to have a highly hydrophobic pocket, used in the binding of vitamin D. This led to the suspicion that some of the acrylodan was not covalently bound, but held by hydrophobic interactions.

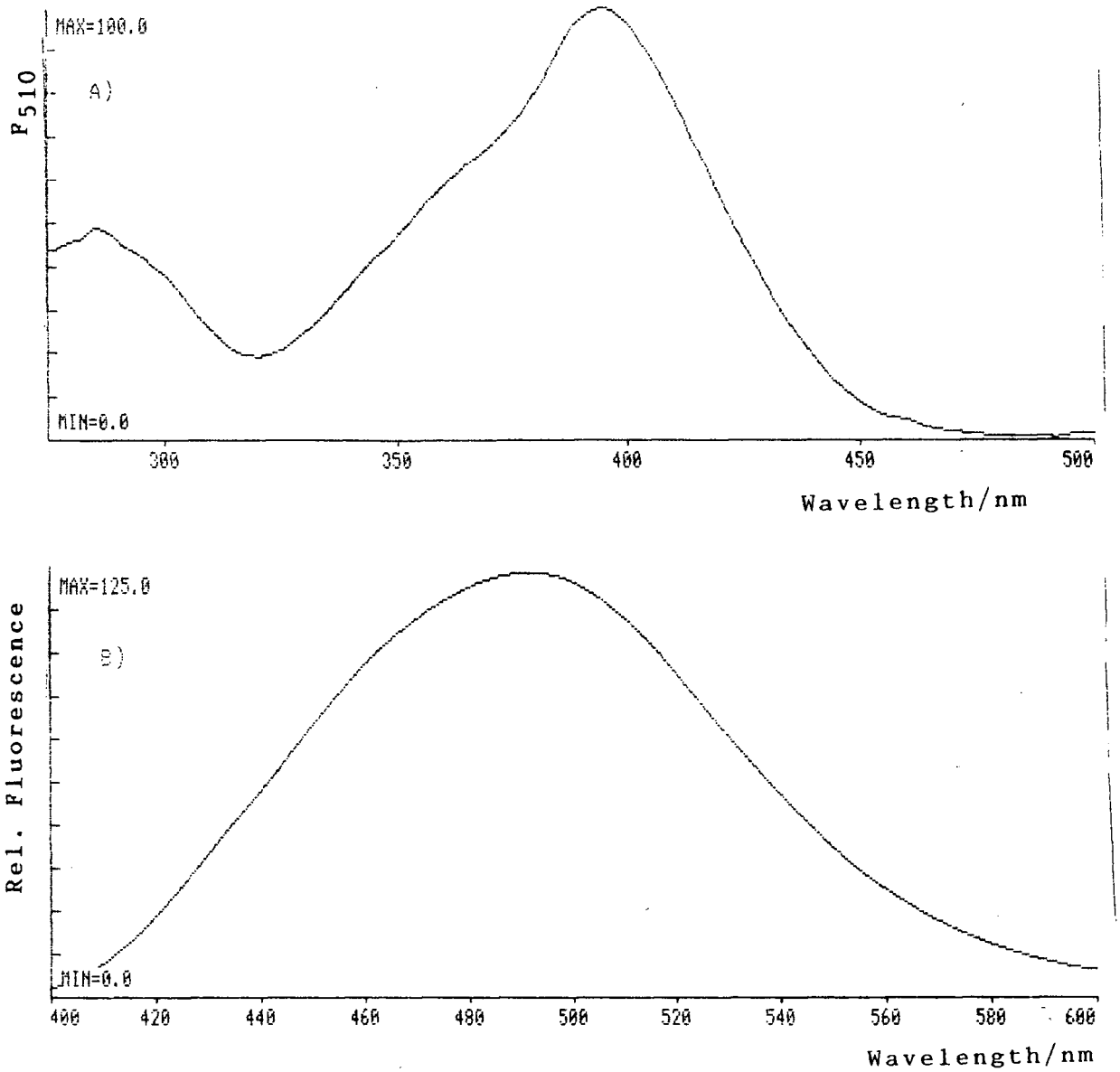

Fig 31: Fluorescence spectra of acrylodan-DBP (5:1 labeled) at 20 °C.
A) Excitation spectrum, emission at 510 nm.
B) Emission spectrum, excitation at 365 nm.

On addition of DTT (5 mM) to the acrylodan-DBP a large red shift in the emission maximum is immediately seen (fig 32). The increase in intensity is most likely due to the hydrophobically bound acrylodan reacting with DTT, as acrylodan has low fluorescence intensity (Pendergast et al., 1983). The red shift could be due to the release of this

acrylodan-DTT into the solvent. This last point is supported by the observation that, on dialysis against 20 mM MOPS, 2 mM DTT, pH 7.3 (3 changes in 36 h), this mixture had a much diminished acryodan emission spectra, and the new extent of labeling of acrylodan-DBP was the calculated to be 0.35 ± 0.29 acrylodans per DBP. Furthermore, when this DTT-treated acrylodan-DBP was run on an SDS polyacrylamide electrophoretic gel, all the acrylodan fluorescence was seen to migrate with DBP and none was detected at the dye front. This suggests that the remaining acrylodan was covalently bound. It was this DTT-treated acrylodan-DBP that was used in subsequent experiments, after it had been dialysed extensively against a non-DTT containing buffer (20 mM MOPS, pH 7.3, 3 changes in 36 h).

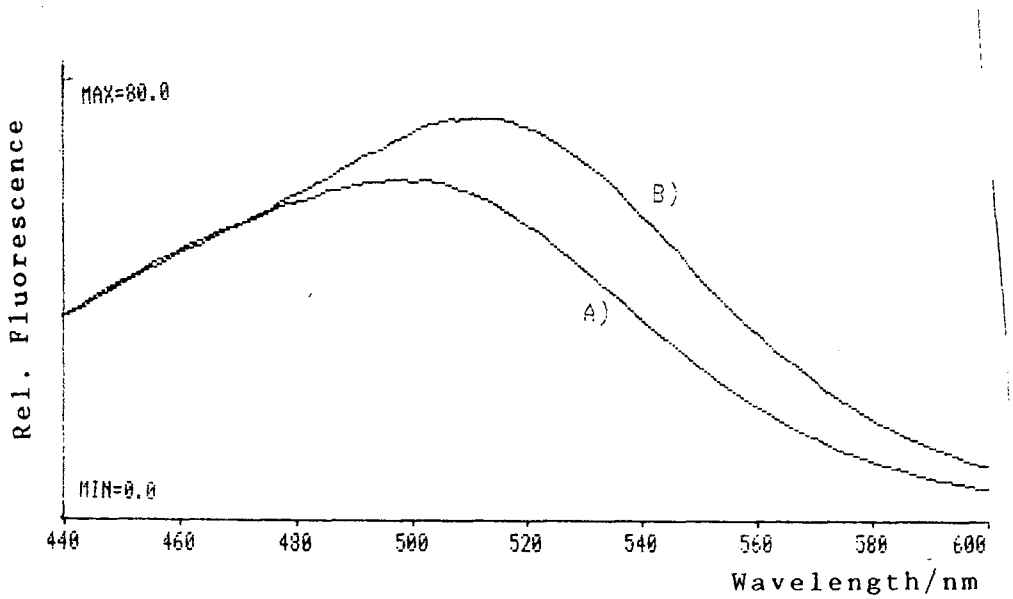

Fig 32: The effect of DTT on the emission spectrum of acrylodan-DBP (5:1 labeled), excitation at 365 nm at 20 °C.
A) acrylodan-DBP alone.
B) acrylodan-DBP + 5 mM DTT.

The new emission spectrum had the same shape as the DBP with hydrophobically bound acrylodan although the emission maximum 488 nm, excitation at 365 nm, had moved from 495nm. This is blue shifted relative to an acrylodan-mercaptoethanol adduct (540 nm), and is slightly blue-shifted relative to other proteins: papain, 491 nm; parvalbumin, 498 nm; and carbonic anhydrase 501 nm (Pendergast et al., 1983), suggesting that the acrylodan is in a very hydrophobic environment.

3.3.2 Interaction of Acryodan-DBP with Actin

On addition of actin to acrylodan-DBP in a 1:1 ratio, there is a red-shift in the fluorescence emission maximum from 488 nm to 494 nm (fig 33), combined with a reduction in

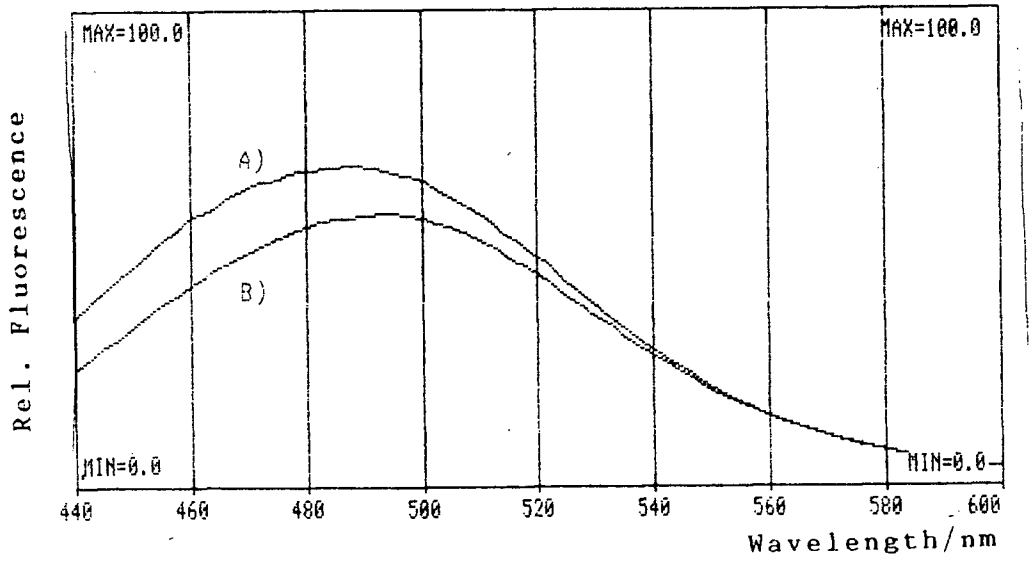

Fig 33: The effect of actin binding on the emission spectrum of acrylodan-DBP (0.35:1 labeled), excitation at 365 nm at 20 °C. A) acrylodan-DBP alone
B) acrylodan-DBP + actin (1:1)

intensity, indicating that the acrylodan has moved to a less hydrophobic environment. These effects can be explained by actin binding at a site different than that labeled with acrylodan and producing a conformational change in DBP which exposes the acrylodan probe to the solvent.

3.3.3 Effect of DTT on Fluorescence of Acrylodan covalently Bound to DBP

Two acrylodan-DBP samples equilibrated against different buffers, one in 20 mM Tris-HCl, pH 8.0 and the other initially incubated for 2 h in the same buffer but containing 5 mM DTT, and subsequently dialysed against 2 mM DTT, 20 mM Tris-HCl, pH 8.0 (3 changes over 36 h). The absorbances at 280 nm of the two samples were within 2% of each other. The emission maximum for the acrylodan-DBP sample that had been incubated with DTT was slightly blue-shifted (fig 34) to 483 nm and its intensity enhanced 30%,

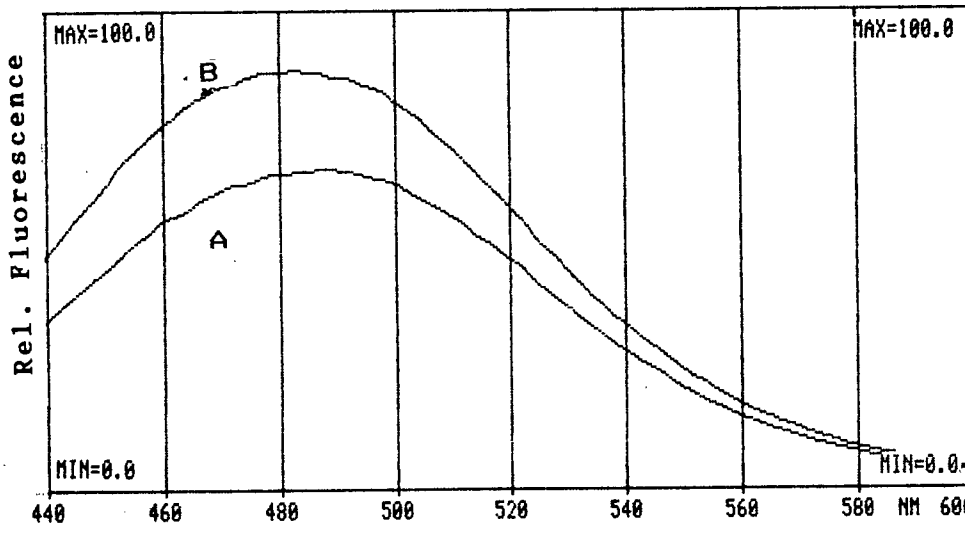

Fig 34: The effect of DTT on the emission spectrum of acrylodan-DBP (0.35:1 labeled), excitation at 365 nm, 20 °C.
A) acrylodan-DBP alone
B) acrylodan-DBP + DTT

implying that the acrylodan had moved into a more hydrophobic environment. A possible explanation for this is that the disulphide bonds present in the protein introduce a certain amount of strain into the structure, and this strain is released when the disulphide bonds are cleaved. The ensuing conformational change affects the acrylodan probe.

Part 4: Conclusions

Horse plasma DBP closely resembles other plasma DBP's. It is a tryptophan-free protein of molecular mass 53,000 daltons that is able to bind actin and block its polymerization. Published purification schemes for other plasma DBP species yielded only partly pure horse plasma DBP. A final anion exchange HPLC step was required to achieve purity.

CD and fluorescence investigations have revealed the importance of the disulphide bonds to the thermal stability of DBP. Without these disulphide bonds, the protein would be significantly unfolded (30%) at body temperature. Furthermore, the disulphide bonds guide the refolding of heated DBP to a functional state on cooling.

DBP can be covalently labeled with acrylodan to produce a highly fluorescent product that is sensitive to the binding of actin and to the state of oxidation of the protein sulfhydryl groups. This initial study of acrylodan-DBP should be extended to identify the site of labeling using peptide mapping techniques and by application of other fluorescence methods

(polarization, quenching, energy transfer) to better characterize the site of labeling and how it is affected by the binding of actin.

The fact that acrylodan appears to bind, in part, non-covalently to DBP suggests a study using a hydrophobic probe (such as 2-(*N*-methylanilino)naphthalene-6-sulphonic acid, Seliskar and Brand, 1979). Fluorescence properties of the bound probe would provide further structural information about the hydrophobic pocket on DBP that is expected from its sequence analogy with serum albumin and that probably is associated with binding vitamin D.

References

1 Berggård, I., Cleve, H., and Bearn, A.G. (1964) Clin. Chim. Acta 10, 1-11.

2 Borke, J.L., Litwiller, R.D., Bell, M.P., Fass, D.N., McKean, D.J., and Kumar, R. (1989) Int. J. Biochem. 20, 1343-1349.

3 Bouillon, R., van Baelen, H., Rombauts, W., and de Moor, P. (1977) J. Biol Chem. 253, 4426-4431.

4 Bouillon, R., van Baelen, H., and de Moor, P. (1986) Binding Proteins of Steriod Hormones. Colloque NSERM/John Libbey Eurotext Ltd. 149, 333-356.

5 Chapuis-Cellier, C., Gianazza, E., and Arnaud, P. (1982) Biochim. Biophys. Acta 709, 353-357.

6 Chen, Y.H., Yang, J.T., and Martinez, H.M. (1972) Biochem. 11, 4120-4131.

7 Cooke, N.E. (1986) J. Biol. Chem. 261, 3441-3450.

8 Cooke, N.E., and Haddad, J.G. (1989) Endocrine Rev. 10, 294-307.

9 Cooper, J.A., Walker, S.B., and Pollard, T.D. (1983) J. Muscle Res. Cell Motility 4, 253-262.

10 Côté, G.P., and Smillie, L.B. (1981) J. Biol. Chem. 256, 7257-7261.

11 Coué, M., Constans, J., and Olmucki, A. (1986) Eur. J. Biochem. 160, 273-277.

12 Creighton, T.E. (1989) Protein Structure a Practical Approach. Oxford Uni. Press 251-284.

13 Daiger, S.P., Schanfield, M.S., and Cavalli-Sforza, L.L. (1975) Proc. Natl. Acad. Sci. USA. 72, 2076-2080.

14 Dueland, S., Blomhoff, R., and Pendersen, J.I. 1990) Biochem. J. 721-725.

15 Ena, J.M., Esterban, C., Perez, M.D., Uriel, J., and Calvo, M. (1989) Biochem. Int. 19, 1-7.

16 Freifelder, D. (1976) Physical Biochemistry. W.H. Freeman and Co. 444-474.

17 Gianazza, E., and Arnaud, P. (1982) Biochem. J. 203, 637-641.

18 Gill, S.C., and von Hippel, P.H. (1989) Anal. Biochem. 182, 319-326.

19 Goldschmidt-Clermont, P.J., Williams, M.H., and Galbraith, R.M. (1987) Biochem. Biophys. Res. Com. 146, 611-617.

20 Haddad, J.G., Harper, K.D., Guoth, M., Pietra, G.G., and Sanger, S.W. (1990) Proc Natl. Acad. Sci. USA. 87, 1381-1385.

21 Hirschfeld, J. (1959) Acta. Pathol. Microbiol. Scand. 47, 160-168.

22 Hirschfeld, J. (1962) Prog. Allergy. 6, 155-186.

23 Janmey, P.A., and Lind, S.E. (1987) Blood 70, 524-530.

24 Janmey, P.A., Stossel, T.P., and Lind, S.E. (1986) Biochem. Biophys. Res. Com. 136, 72-79.

25 Kuwajima, K. (1989) Protiens: Structure, Function and Genetics 6, 87-103.

26 Kawakami, M., and Goodmann, D.S. (1981) Biochem. 20, 5881-5887.

27 Korn, E.D. (1982) Physiol. Rev. 62, 672-737.

28 Laemmli, U.K. (1970) Nature. 227, 680-685.

29 Lehrer, S.S., and Ishii, Y. (1988) Biochem. 27, 5899-5906.

30 Lind, S.E., Smith, B.B., Janmey, P.A., and Stossel, T.P. (1986) J. Clin. Invest. 78, 736-742.

31 Link, R.P., Perlman, K.L., Pierce, E.A., Schnoes, H.K., and DeLuca, H.F. (1986) Anal. Biochem. 157, 262-269.

32 Marriott, G., Zechel, K., and Jovin, T.M. (1988) Biochem. 27, 6214-6220.

33 Nielsen, J.C., Nerstrom, B., and Feldbo, M. (1963) Acta Pathol. Microbiol. Scand. 58, 264-271.

34 Nozaki, Y. (1990) Arch. Biochem. Biophys. 277, 324-33.

35 Pendergast, F.G., Meyer, M., Carlson, G.L., Iida, S., and Potter, J.D. (1983) J. Biol. Chem. 258, 7541-7544.

36 Pollard, T.D., and Craig, S.W. (1982) TIBS 7, 55-58.

37 Pötsch-Schneider, L., and Klein, H. (1988) Electrophoresis 9, 602-605.

38 Safer, D. (1989) Anal. Biochem. 178, 32-37.

39 Seliskan, C.J., and Brand, L. (1971) J. Amer. Chem. Soc. 93, 5405-5420.

40 Spudich, J.A., and Watt, S. (1971) J. Biol. Chem. 246, 4866-4871.

41 Stryer, L. (1981) Biochemistry. W.H. Freeman and Co., 2nd ed. 815-837.

42 Thomas, W.C., Morgan, H.G., Conners, T.B., Haddock, L., Bills, C.E., and Howard, J.E. (1959) J. Clin. Invest. 38, 1078-1085.

43 Tuzimura, K., Konno, T., Meguro, H., Hatano, M., Marakami, T., Kashiwabara, K., Saito, K., Kondo, Y., and Suzuki, T.M. (1977) Anal. Biochem. 81, 167-174.

44 Van Baelen, H., Bouillon, R., and de Moor, P. (1980) J. Biol. Chem. 255, 2270-2272.

45 Van Baelen, H., and Bouillon, R. (1986) Binding Proteins of Steroid Hormones. Colloque NSERM/John Libbey Eurotext Ltd. 149, 63-83.

46 Way, M., and Weeds, A. (1990) Nature 344, 292-294.